Simulating the effect of tillage practices with the global ecosystem model LPJmL (version 5.0-tillage)

Femke Lutz[1,2*] and Tobias Herzfeld[1*], Jens Heinke[1], Susanne Rolinski[1], Sibyll Schaphoff[1], Werner von Bloh[1], Jetse J. Stoorvogel[2], Christoph Müller[1]

[1]Potsdam Institute for Climate Impact Research (PIK), Member of the Leibniz Association
P.O. Box 60 12 03, D-14412 Potsdam, Germany
[2] Wageningen University, Soil Geography and Landscape Group, PO Box 47, 6700 AA Wageningen, The Netherlands.

*Shared lead authorship

Correspondence to: Femke.Lutz@pik-potsdam.de

Abstract. The effects of tillage on soil properties, crop productivity, and global greenhouse gas emissions have been discussed in the last decades. Global ecosystem models have limited capacity to simulate the various effects of tillage. With respect to the decomposition of soil organic matter, they either assume a constant increase due to tillage, or they ignore the effects of tillage. Hence, they do not allow for analyzing the effects of tillage and cannot evaluate, for example, reduced-tillage or no-till as mitigation practices for climate change. In this paper, we describe the implementation of tillage related practices in the global ecosystem model LPJmL. The extended model is evaluated against reported differences between tillage and no-till management on several soil properties. To this end, simulation results are compared with published meta-analysis on tillage effects. In general, the model is able to reproduce observed tillage effects on global, as well as regional patterns of carbon and water fluxes. However, modelled N-fluxes deviate from the literature and need further study. The addition of the tillage module to LPJmL5 opens opportunities to assess the impact of agricultural soil management practices under different scenarios with implications for agricultural productivity, carbon sequestration, greenhouse gas emissions and other environmental indicators.

1 Introduction

Agricultural fields are tilled for various purposes, including seedbed preparation, incorporation of residues and fertilizers, water management and weed control. Tillage affects a variety of biophysical processes that affect the environment, such as greenhouse gas emissions or soil carbon sequestration and can influence various forms of soil degradation (e.g. wind-, water- and tillage-erosion) (Armand et al., 2009; Govers et al., 1994; Holland, 2004). Reduced-tillage or no-till is being promoted as a strategy to mitigate greenhouse gas (GHG) emissions in the agricultural sector (Six et al., 2004; Smith et al., 2008). However, there is an ongoing long-lasting debate about tillage and no-till effects on soil organic carbon (SOC) and GHG emissions (e.g. Lugato et al., 2018). In general, reduced-tillage and no-till tend to increase SOC storage through a reduced decomposition and consequently reduces GHG emissions (Chen et al., 2009; Willekens et al., 2014). However, discrepancies exist on the effectiveness of reduced tillage or no-till on GHG emissions. For instance, Abdalla et al. (2016) found in a meta-analyses that on average no-till systems reduce CO_2 emissions by 21% compared to conventional tillage, whereas Oorts et al. (2007) found that CO_2 emissions from no-till systems increased by 13% compared to conventional tillage, and Aslam et al. (2000) found only minor differences in CO_2 emissions. These

42   discrepancies are not surprising as tillage affects a complex set of biophysical factors, such as soil moisture and

43   soil temperature (Snyder et al., 2009), which drive several soil processes, including the carbon and nitrogen

44   dynamics, and crop performance. Moreover, other factors such as management practices (e.g. fertilizer

45   application and residue management) and climatic conditions have been shown to be important confounding

46   factors (Abdalla et al., 2016; Oorts et al., 2007; van Kessel et al., 2013). For instance Oorts et al. (2007)

47   attributed the higher CO_2 emissions under no-till to higher soil moisture and decomposition of crop litter on top

48   of the soil. Van Kessel et al. (2013) found that N_2O emissions were smaller under no-till in dry climates and that

49   the depth of fertilizer application was important. Finally, Abdalla et al. (2016) found that no-till effects on CO_2

50   emissions are most effective in dryland soils.

51   In order to upscale this complexity and to study the role of tillage for global biogeochemical cycles, crop

52   performance and mitigation practices, the effects of tillage on soil properties need to be represented in global

53   ecosystem models. Although tillage is already implemented in other ecosystem models in different levels of

54   complexity (Lutz et al., 2019; Maharjan et al., 2018), tillage practices are currently underrepresented in global

55   ecosystem models that are used for biogeochemical assessments. In these, the effects of tillage are either ignored,

56   or represented by a simple scaling factor of decomposition rates. Global ecosystem models that ignore the effects

57   of tillage include for example JULES (Best et al., 2011; Clark et al., 2011) , the Community Land Model (Levis

58   et al., 2014; Oleson et al., 2010) PROMET (Mauser and Bach, 2009) and the Dynamic Land Ecosystem Model

59   (DLEM) (Tian et al., 2010). The models in which the effects of tillage are represented as an increase in

60   decomposition include LPJ-GUESS (Olin et al., 2015; Pugh et al., 2015) and ORCHIDEE-STICS (Ciais et al.,

61   2011).

62   The objective of this paper is to 1) extend the Lund Potsdam Jena managed Land (LPJmL5) model (von Bloh

63   et al., 2018), so that the effects of tillage on biophysical processes and global biogeochemistry can be

64   represented and studied and 2) evaluate the extended model against data reported in meta-analyses by using a set

65   of stylized management scenarios. This extended model version allows for quantifying the effects of different

66   tillage practices on biogeochemical cycles, crop performance and for assessing questions related to agricultural

67   mitigation practices. Despite uncertainties in the formalization and parameterization of processes, the processed-

68   based representation allows for enhancing our understanding of the complex response patterns as individual

69   effects and feedbacks can be isolated or disabled to understand their importance. To our knowledge, some crop

70   models that have been used at the global scale, EPIC (Williams et al., 1983) and DSSAT (White et al., 2010),

71   have similarly detailed representations of tillage practices, but models used to study the global biogeochemistry

72   (Friend et al., 2014) have no or only very coarse representations of tillage effects.

73   **2 Tillage effects on soil processes**

74   Tillage affects different soil properties and soil processes, resulting in a complex system with various

75   feedbacks on soil water, temperature, carbon (C) and nitrogen (N) related processes (Fig. 1). The effect of tillage

76   has to be implemented and analyzed in conjunction with residue management as these management practices are

77   often inter-related (Guérif et al., 2001; Strudley et al., 2008). The processes that were implemented into the

78   model were chosen based on the importance of the process and its compatibility with the implementation of

79   other processes within the model. Those processes are visualized in Fig. 1 with solid lines; processes that have

80   been ignored in this implementation are visualized with dotted lines. To illustrate the complexity, we here

81 describe selected processes in the model affected by tillage and residue management, using the numbered lines in
82 Fig. 1.

83   With tillage, surface litter is incorporated into the soil [1] and increases the soil organic matter (SOM)
84 content of the tilled soil layer [2] (Guérif et al., 2001; White et al., 2010), while tillage also decreases the bulk
85 density of this layer [3] (Green et al., 2003). An increase in SOM positively affects the porosity [4] and therefore
86 the soil water holding capacity (whc) [5] (Minasny and McBratney, 2018). Tillage also affects the whc by
87 increasing porosity [6] (Glab and Kulig, 2008). A change in whc affects several water-related processes through
88 soil moisture [7]. For instance, changes in soil moisture influence lateral runoff [8] and leaching [9] and affect
89 infiltration. A wet (saturated) soil for example decreases infiltration [10], while infiltration can be enhanced if
90 the soil is dry (Brady and Weil, 2008). Soil moisture affects primary production as it determines the amount of
91 water which is available for the plants [11] and changes in plant productivity again determine the amount of
92 residues left at the soil surface or to be incorporated into the soil [1] (feedback not shown).

93   The presence of crop residues on top of the soil (referred to as "surface litter" hereafter) enhances water
94 infiltration into the soil [12] (Guérif et al., 2001; Jägermeyr et al., 2016; Ranaivoson et al., 2017), and thus
95 increases soil moisture [13]. That is because surface litter limits soil crusting, can constitute preferential
96 pathways for water fluxes and slows lateral water fluxes at the soil surface so that water has more time to
97 infiltrate (Glab and Kulig, 2008). Consequently, surface litter reduces surface runoff [14] (Ranaivoson et al.,
98 2017). Surface litter also intercepts part of the rainfall [15], reducing the amount of water reaching the soil
99 surface, but also lowers soil evaporation [16] and thus reduces unproductive water losses to the atmosphere (Lal,
100 2008; Ranaivoson et al., 2017). Surface litter also reduces the amplitude of variations in soil temperature [17]
101 (Enrique et al., 1999; Steinbach and Alvarez, 2006). The soil temperature is strongly related to soil moisture
102 [18], through the heat capacity of the soil, i.e. a relatively wet soil heats up much slower than a relatively dry soil
103 (Hillel, 2004). The rate of SOM mineralization is influenced by changes in soil moisture [19] and soil
104 temperature [20] (Brady and Weil, 2008). The rate of mineralization affects the amount of CO_2 emitted from
105 soils [21] and the inorganic N content of the soil. Inorganic N can then be taken up by plants [22], be lost as
106 gaseous N [23], or transformed into other forms of N. The processes of nitrate (NO_3^-) leaching, nitrification,
107 denitrification, mineralization of SOM and immobilization or mineral N forms are explicitly represented in the
108 model (von Bloh et al., 2018). The degree to which soil properties and processes are affected by tillage mainly
109 depends on the tillage intensity, which is a combination of tillage efficiency and mixing efficiency (in detail
110 explained in chapter 3.2 and 3.5.2). Tillage has a direct effect on the bulk density of the tilled soil layer. The type
111 of tillage determines the mixing efficiency, which affects the amount of incorporating residues into the soil. Over
112 time, soil properties reconsolidate after tillage, eventually returning to pre-tillage states. The speed of
113 reconsolidation depends on soil texture and the kinetic energy of precipitation (Horton et al., 2016).

114   This implementation mainly focuses on two processes directly affected by tillage: 1) the incorporation of
115 surface litter associated with tillage management and the subsequent effects (Fig. 1, arrow 1 and following
116 arrows), 2) the decrease in bulk density and the subsequent effects of changed soil water properties (Fig. 1, e.g.
117 arrow 3 and following arrows). In order to limit model complexity and associated uncertainty, tillage effects that
118 are not directly compatible with the original model structure, such as subsoil compaction, or require very high
119 spatial resolution, are not taken into account in this initial tillage implementation, despite acknowledging that
120 these processes can be important.
121   *[Fig. 1]*

3 Implementation of tillage routines into LPJmL

3.1 LPJmL model description

The tillage implementation described in this paper was introduced into the dynamical global vegetation, hydrology and crop growth model LPJmL. This model was recently extended to also cover the terrestrial N cycle, accounting for N dynamics in soils and plants and N limitation of plant growth (LPJmL5; von Bloh et al., 2018). Previous comprehensive model descriptions and developments are described by Schaphoff et al. (2018a). The LPJmL model simulates the C, N and water cycles by explicitly representing biophysical processes in plants (e.g. photosynthesis) and soils (e.g. mineralization of N and C). The water cycle is represented by the processes of rain water interception, soil and lake evaporation, plant transpiration, soil infiltration, lateral and surface runoff, percolation, seepage, routing of discharge through rivers, storage in dams and reservoirs and water extraction for irrigation and other consumptive uses.

In LPJmL5, all organic matter pools (vegetation, litter and soil) are represented as C pools and the corresponding N pools with variable C:N ratios. Carbon, water and N pools in vegetation and soils are updated daily as the result of computed processes (e.g. photosynthesis, autotrophic respiration, growth, transpiration, evaporation, infiltration, percolation, mineralization, nitrification, leaching; see von Bloh et al. (2018) for the full description). Litter pools are represented by the above-ground pool (e.g. crop residues, such as leaves and stubbles) and the below-ground pool (roots). The litter pools are subject to decomposition, after which the humified products are transferred to the two SOM pools that have different decomposition rates (Fig. S1A in the Supplement). The fraction of litter which is harvested from the field can range between almost fully harvested or none, when all litter is left on the field (90%, Bondeau et al., 2007). In the soil, pools of inorganic reactive N forms (NH_4^+, NO_3^-) are also considered. Each organic soil pool consists of C and N pools and the resulting C:N ratios are flexible. Soil C:N ratios are considerably smaller than those of plants as immobilization by microorganisms concentrates N in SOM. In LPJmL, a soil C:N ratio of 15 is targeted by immobilization for all soil types (von Bloh et al., 2018). The SOM pools in the soil consist of a fast pool with a turnover time of 30 years, and a slow pool with a 1000 year turnover time (Schaphoff et al., 2018a). Soils in LPJmL5 are represented by five hydrologically active layers, each with a distinct layer thickness. The first soil layer, which is mostly affected by tillage, is 0.2 m thick. The following soil layers are 0.3, 0.5, 1.0 and 1.0 m thick, respectively, followed by a 10.0 m bedrock layer, which serves as a heat reservoir in the computation of soil temperatures (Schaphoff et al. 2013).

LPJmL5 has been evaluated extensively and demonstrated good skills in reproducing C,- water and N fluxes in both agricultural and natural vegetation on various scales (Bloh et al., 2018; Schaphoff et al., 2018b).

3.2 Litter pools and decomposition

In order to address the residue management effects of tillage, the original above-ground litter pool is now separated into an incorporated litter pool ($C_{litter,inc}$) and a surface litter pool ($C_{litter,surf}$) for carbon, and the corresponding pools ($N_{litter,inc}$) and ($N_{litter,surf}$) for nitrogen (Fig. S1B in the Supplement). Crop residues not collected from the field are transferred to the surface litter pools. A fraction of residues from the surface litter pool is then partially or fully transferred to the incorporated litter pools, depending on the tillage practice;

160      $C_{litter,inc,t+1} = C_{litter,inc,t} + C_{litter,surf,t} \cdot TL$, for carbon , and   (1)

161      $N_{litter,inc,t+1} = N_{litter,inc,t} + N_{litter,surf,t} \cdot TL$, for nitrogen.

162

163   The $C_{litter,surf}$ and $N_{litter,surf}$ pools are reduced accordingly:

164

165      $C_{litter,surf,t+1} = C_{litter,surf,t} \cdot (1 - TL)$,   (2)

166      $N_{litter,surf,t+1} = N_{litter,surf,t} \cdot (1 - TL)$,

167

168   where $C_{litter,inc}$ and $N_{litter,inc}$ is the amount of incorporated surface litter C and N in g m^{-2} at time step t (days).

169   The parameter TL is the tillage efficiency, which determines the fraction of residues that is incorporated by

170   tillage (0-1). To account for the vertical displacement of litter through bioturbation under natural vegetation and

171   under no-till conditions, we assume that 0.1897% of the surface litter pool is transferred to the incorporated litter

172   pool per day (equivalent to an annual bioturbation rate of 50%).

173   The litter pools are subject to decomposition. The decomposition of litter depends on the temperature and

174   moisture of its surroundings. The decomposition of the incorporated litter pools depends on soil moisture and

175   temperature of the first soil layer (as described by von Bloh et al., 2018), whereas the decomposition of the

176   surface litter pools depends on the litter's moisture and temperature, which are approximated by the model. The

177   decomposition rate of litter ($rdecom$ in g C m^{-2} day^{-1}) is described by first-order kinetics, and is specific for

178   each "plant functional type" (PFT), following Sitch et al. (2003);

179

180      $rdecom_{(PFT)} = 1 - exp(-\frac{1}{\tau_{10(PFT)}} \cdot g(T_{surf}) \cdot F(\Theta))$,   (3)

181

182   where τ_{10} is the mean residence time for litter and $F(\Theta)$ and $g(T_{surf})$ are response functions of the decay rate to

183   litter moisture and litter temperature (T_{surf}) respectively. The response function to litter moisture $F(\Theta)$ is

184   defined as;

185

186      $F(\Theta) = 0.0402 - 5.005 \cdot \Theta^3 + 4.269 \cdot \Theta^2 + 0.7189 \cdot \Theta$,   (4)

187

188   where, Θ is the volume fraction of litter moisture which depends on the water holding capacity of the surface

189   litter (whc_{surf}), the fraction of surface covered by litter (f_{surf}), the amount of water intercepted by the surface

190   litter (I_{surf}) (chapter 3.3.1) and lost through evaporation E_{surf} (chapter 3.3.3).

191   The temperature function $g(T_{surf})$ describes the influence of temperature of surface litter on decomposition

192   (von Bloh et al., 2018);

193

194      $g(T_{surf}) = exp(308.56 \cdot (\frac{1}{66.02} - \frac{1}{(T_{surf}+56.02)}))$,   (5)

195

196   where T_{surf} is the temperature of surface litter (chapter 3.4).

197   A fixed fraction (70%) of the decomposed $C_{litter,surf}$ is mineralized, i.e., emitted as CO_2, whereas the remaining

198   humified C is transferred to the soil C pools, where it is then subject to the soil decomposition rules as described

199   by von Bloh et al. (2018) and Schaphoff et al. (2018a). The mineralized N (also 70% of the decomposed litter) is

200   added to the NH$_4^+$pool of the first soil layer, where it is subjected to further transformations (von Bloh et al.,

201   2018), whereas the humified organic N (30% of the decomposed litter) is allocated to the different organic soil N

202   pools in the same shares as the humified C. In order to maintain the desired C:N ratio of 15 within the soil (von

203   Bloh et al., 2018), the mineralized N is subject to microbial immobilization, i.e., the transformation of mineral N

204   to organic N directly reverting some of the N mineralization in the soil.

205   The presence of surface litter influences the soil water fluxes and soil temperature of the soil (see 3.3 and

206   3.4), and therefore affects the decomposition of the soil carbon and nitrogen pools, including the transformations

207   of mineral N forms. Nitrogen fluxes such as N$_2$O from nitrification and denitrification for instance, are partly

208   driven by soil moisture (von Bloh et al., 2018):

209

210   $$F_{N2O,nitrification,l} = K_2 \cdot K_{max} \cdot F_1(T_l) \cdot F_1(W_{sat,l}) \cdot F(pH) \cdot NH_{4,l}^+ \text{ for nitrification, and} \tag{6}$$

211   $$F_{N2O,denitrification,l} = r_{mx2} \cdot F_2(W_{sat,l}) \cdot F_2(T_l, C_{org}) \cdot NO_{3,l}^- \text{ for denitrification.}$$

212

213   Where $F_{N2O,nitrification}$ and $F_{N2O,denitrification}$ are the N$_2$O flux related to nitrification and denitrification

214   respectively in gN m^{-2} d^{-1} in layer l. K_2 is the fraction of nitrified N lost as N$_2$O ($K_2 = 0.02$), K_{max} is the

215   maximum nitrification rate of NH$_4^+$ ($K_{max} = 0.1\, d^{-1}$). $F_1(T_l)$, $F_1(W_{sat,l})$, are response functions of soil

216   temperature and water saturation respectively, that limit the nitrification rate. $F(pH)$ is the function describing

217   the response of nitrification rates to soil pH and $NH_{4,l}^+$ and $NO_{3,l}^-$ the soil ammonium and nitrate concentration in

218   gN m^{-2} respectively. $F_2(T_l, C_{org})$, $F_2(W_{sat,l})$ are reaction for soil temperature, soil carbon and water saturation

219   and r_{mx2} is the fraction of denitrified N lost as N$_2$O (11%, the remainder is lost as N$_2$). For a detailed description

220   of the N related processes implemented in LPJmL, we refer to von Bloh et al. (2018).

221   **3.3 Water fluxes**

222   **3.3.1 Litter interception**

223   Precipitation and applied irrigation water in LPJmL5 is partitioned into interception, transpiration, soil

224   evaporation, soil moisture and runoff (Jägermeyr et al., 2015). To account for the interception and evaporation of

225   water by surface litter, the water can now also be captured by surface litter through litter interception (I_{surf}) and

226   be lost through litter evaporation, subsequently infiltrates into the soil and/or forms surface runoff. Litter

227   moisture (Θ) is calculated in the following way:

228

229   $$\Theta_{t+1} = min(whc_{surf} - \Theta_{(t)}, I_{surf} \cdot f_{surf}). \tag{7}$$

230

231   f_{surf} is calculated by adapting the equation from Gregory (1982) that relates the amount of surface litter (dry

232   matter) per m^2 to the fraction of soil covered;

233

234   $$f_{surf} = 1 - exp^{-A_m \cdot OM_{litter,surf}}, \tag{8}$$

235

236   where $OM_{litter,surf}$ is the total mass of dry matter surface litter in g m^{-2} and A_m is the area covered per mass of

237   crop specific residue (m^2 g^{-1}). The total mass of surface litter is calculated assuming a fixed C to organic matter

238   ratio of 2.38 ($CF_{OM,litter}$), based on the assumption that 42% of the organic matter is C, as suggested by Brady

239   and Weil (2008):

240

241    $$OM_{litter,surf} = C_{litter,surf} \cdot CF_{OM,litter},\qquad(9)$$

242

243   where $C_{litter,surf}$ is the amount of C stored in the surface litter pool in g C m⁻². We apply the average value of

244   0.004 for A_m from Gregory (1982) to all materials, neglecting variations in surface litter for different materials.

245   whc_{surf} (mm) is the water holding capacity of the surface litter and is calculated by multiplying the litter mass

246   with a conversion factor of 2 10⁻³ mm kg⁻¹ ($OM_{litter,surf}$) following Enrique et al. (1999).

3.3.2 Soil infiltration

248   The presence of surface litter enhances infiltration of precipitation or irrigation water into the soil, as soil

249   crusting is reduced and preferential pathways are affected (Ranaivoson et al., 2017). In order to account for

250   improved infiltration with the presence of surface litter, we follow the approach by Jägermeyr et al. (2016),

251   which has been developed for implementing in situ water harvesting, e.g. by mulching in LPJmL. The

252   infiltration rate (In in mm d⁻¹) depends on the soil water content of the first layer and the infiltration

253   parameter p;

254

255    $$In = prir \cdot \sqrt[p]{1 - \frac{W_a}{W_{sat,l=1} - W_{pwp,l=1}}},\qquad(10)$$

256

257

258   where $prir$ is the daily precipitation and applied irrigation water in mm, W_a the available soil water content in

259   the first soil layer, and $W_{sat,l=1}$ and $W_{pwp,l=1}$ the soil water content at saturation and permanent wilting point of

260   the first layer in mm. By default $p = 2$, but four different levels are distinguished ($p = 3, 4, 5, 6$) by Jägermeyr

261   et al. (2016), in order to account for increased infiltration based on the management intervention. To account for

262   the effects of surface litter, we here scale the infiltration parameter p between 2 and 6, based on the fraction of

263   surface litter cover (f_{surf});

264

265    $$p = 2 \cdot (1 + f_{surf} \cdot 2)\qquad(11)$$

266

267   Surplus water that cannot infiltrate forms surface runoff and enters the river system.

3.3.3 Litter and soil evaporation

269   Evaporation (E_{surf}, in mm) from the surface litter cover (f_{surf}), is calculated in a similar manner as evaporation

270   from the first soil layer (Schaphoff et al., 2018a). Evaporation depends on the vegetation cover (f_v), the radiation

271   energy for the vaporization of water (PET) and the water stored in the surface litter that is available to evaporate

272   (ω_{surf}) relative to whc_{surf}. Here, also f_{surf} is taken into account so that the fraction of soil uncovered is subject

273   to soil evaporation as described in Schaphoff et al. (2018a);

274

275 $$E_{surf} = PET \cdot \alpha \cdot \max(1 - f_v, 0.05) \cdot \omega_{surf}^2 \cdot f_{surf}, \tag{12}$$

276

277 $$\omega_{surf} = \Theta/whc_{surf}, \tag{13}$$

278

279 where PET is calculated based on the theory of equilibrium evapotranspiration (Jarvis and McNaughton, 1986)

280 and α the empirically derived Priestley-Taylor coefficient ($\alpha = 1.32$) (Priestley and Taylor, 1972).

281   The presence of litter at the soil surface reduces the evaporation from the soil (E_{soil}). E_{soil} (mm) corresponds

282 to the soil evaporation as described in Schaphoff et al. (2018a), and depends on the available energy for

283 vaporization of water and the available water in the upper 0.3 m of the soil (ω_{evap}). However, with the

284 implementation of tillage, the fraction of f_{surf} now also influences evaporation, i.e., greater soil cover (f_{surf})

285 results in a decrease in E_{soil};

286

287 $$E_{soil} = PET \cdot \alpha \cdot \max(1 - f_v, 0.05) \cdot \omega^2 \cdot (1 - f_{surf}) \tag{14}$$

288

289 ω is calculated as the evaporation-available water (ω_{evap}) relative to the water holding capacity in that layer

290 (whc_{evap});

291

292 $$\omega = \min\left(1, \frac{\omega_{evap}}{whc_{evap}}\right), \tag{15}$$

293 where ω_{evap} is all the water above wilting point of the upper 0.3 m (Schaphoff et al., 2018a).

294 **3.4 Heat flux**

295 The temperature of the surface litter is calculated as the average of soil temperature of the previous day (t) of the

296 first layer ($T_{soil,l=1}$ in°C) and actual air temperature ($T_{air,t+1}$ in°C), in the following way:

297

298 $$T_{litter,surf,t+1} = 0.5(T_{air,t+1} + T_{l=1,t}). \tag{16}$$

299

300 Equation (16) is an approximate solution for the heat exchange described by Schaphoff et al. (2013). The new

301 upper boundary condition (T_{upper} in °C) is now calculated by the average of T_{air} and T_{surf} weighted by f_{surf}.

302 With the new boundary condition, the cover of the soil with surface litter diminishes the heat exchange between

303 soil and atmosphere;

304

305 $$T_{upper} = T_{air} \cdot (1 - f_{surf}) + T_{surf} \cdot f_{surf}. \tag{17}$$

306

307 The remainder of the soil temperature computation remains unchanged from the description of Schaphoff et al.

308 (2013).

3.5 Tillage effects on physical properties

3.5.1 Dynamic calculation of hydraulic properties

Previous versions of the LPJmL model used static soil hydraulic parameters as inputs, computed following the pedotransfer function (PTF) by Cosby et al. (1984). Different methods exist to calculate soil hydraulic properties from soil texture and SOM content for different points of the water retention curve (Balland et al., 2008; Saxton and Rawls, 2006; Wösten et al., 1999) or at continuous pressure levels (Van Genuchten, 1980; Vereecken et al., 2010). Extensive reviews of PTFs and their application in Earth system and soil modeling can be found in Van Looy et al. (2017) and Vereecken et al. (2016). We now introduced an approach following the PTF by Saxton and Rawls (2006), which was included in the model in order to dynamically simulate layer-specific hydraulic parameters that account for the amount of SOM in each layer, constituting an important mechanism of how hydraulic parameters are affected by tillage (Strudley et al., 2008).

As such, Saxton and Rawls (2006) define a PTF most suitable for our needs and capable of calculating all the necessary soil water properties for our approach: it allows for a dynamic effect of SOM on soil hydraulic properties, and is also capable of representing changes in bulk density after tillage and was developed from a large number of data points. With this implementation, soil hydraulic properties are now all updated daily. Following Saxton and Rawls (2006), soil water properties are calculated as:

$$\lambda_{pwp,l} = -0.024 \cdot Sa + 0.0487 \cdot Cl + 0.006 \cdot SOM_l + 0.005 \cdot Sa \cdot SOM_l - 0.013 \cdot Cl \cdot SOM_l + 0.068 \cdot Sa \cdot Cl + 0.031, \tag{18}$$

$$W_{pwp,l} = 1.14 \cdot \lambda_{pwp,l} - 0.02, \tag{19}$$

$$\lambda_{fc,l} = -0.251 \cdot Sa + 0.195 \cdot Cl + 0.011 \cdot SOM_l + 0.006 \cdot Sa \cdot SOM_l - 0.027 \cdot Cl \cdot SOM_l + 0.452 \cdot Sa \cdot Cl + 0.299, \tag{20}$$

$$W_{fc,l} = 1.238 \cdot \left(\lambda_{fc,l}\right)^2 \mp 0.626 \cdot \lambda_{fc,l} - 0.015, \tag{21}$$

$$\lambda_{sat,l} = 0.278 \cdot Sa + 0.034 \cdot Cl + 0.022 \cdot SOM_l - 0.018 \cdot Sa \cdot SOM_l - 0.027 \cdot Cl \cdot SOM_l - 0.584 \cdot Sa \cdot Cl + 0.078, \tag{22}$$

$$W_{sat,l} = W_{fc,l} + 1.636 \cdot \lambda_{sat,l} - 0.097 \cdot Sa - 0.064, \tag{23}$$

$$BD_{soil,l} = (1 - W_{sat,l}) \cdot MD. \tag{24}$$

SOM_l is the soil organic matter content in weight percent (%w) of layer l, $W_{pwp,l}$ is the moisture content at the permanent wilting point, $W_{fc,l}$ moisture contents at field capacity, $W_{sat,l}$ is the moisture contents at saturation, $\lambda_{pwp,l}$, $\lambda_{fc,l}$ and $\lambda_{sat,l}$ are the moisture contents for the first solution at permanent wilting point, field capacity and saturation, Sa is the sand content in volume percent (%v), Cl is the clay content in %v, $BD_{soil,l}$ is the bulk density in kg m^{-3}, MD is the mineral density of 2700 kg m^{-3}. For SOM_l, total SOC content is translated into SOM of this layer, following:

$$SOM_l = \frac{CF_{OM,soil} \cdot (C_{fastSoil,l} + C_{slowSoil,l})}{BD_{soil,l} \cdot z_l} \cdot 100, \tag{25}$$

where $CF_{OM,soil}$ is the conversion factor of 2 as suggested by Pribyl (2010), assuming that SOM contains 50% SOC, $C_{fastSoil,l}$ is the fast decaying C pool in kg m^{-2}, $C_{slowSoil,l}$ is the slow decaying C pool in kg m^{-2}, $BD_{soil,l}$ is

the bulk density in kg m^{-3} and z is the thickness of layer l in m. It was suggested by Saxton and Rawls (2006) that the PTF should not be used for SOM content above 8%, so we cap SOM_l at this maximum when computing soil hydraulic properties and thus treated soils with SOM_l content above this threshold as soils with 8% SOM content. Saturated hydraulic conductivity is also calculated following Saxton and Rawls (2006) as:

$$Ks_l = 1930 \cdot \left(W_{sat_{(l)}} - W_{fc_{(l)}}\right)^{3-\phi_l},$$
(26)

$$\phi_l = \frac{\ln(W_{fc,l}) - \ln(W_{pwp,l})}{\ln(1500) - \ln(33)},$$
(27)

where Ks_l is the saturated hydraulic conductivity in mm h^{-1} and ϕ_l is the slope of the logarithmic tension-moisture curve of layer l.

3.5.2 Bulk density effect and reconsolidation

The effects of tillage on BD are adopted from the APEX model by Williams et al. (2015) which is a follow-up development of the EPIC model (Williams et al., 1983). Tillage causes changes in BD of the tillage layer (first topsoil layer of 0.2 m) after tillage. Soil moisture content for the tillage layer is updated using the fraction of change in BD. Ks_l is also updated based on the new moisture content after tillage. A mixing efficiency parameter (mE) depending on the intensity and type of tillage (0-1), determines the fraction of change in BD after tillage. A mE of 0.90 for example represents a full inversion tillage practice, also known as conventional tillage (White et al., 2010). The parameter mE can be used in combination with residue management assumptions to simulate different tillage types. It should be noted that Williams et al. (1983) calculate direct effects of tillage on BD, while we changed the equation accordingly to account for the fraction at which BD is changed.

The fraction of BD change after tillage is calculated the following way:

$$f_{BDtill,t+1} = f_{BDtill,t} - \left(f_{BDtill,t} - 0.667\right) \cdot mE.$$
(28)

Tillage density effects on saturation and field capacity follow Saxton and Rawls (2006):

$$W_{sat,till,l,t+1} = 1 - \left(1 - W_{sat,l,t}\right) \cdot f_{BDtill,t+1},$$
(29)

$$W_{fc,till,l,t+1} = W_{fc,l,t} - 0.2 \cdot (W_{sat,l,t} - W_{sat,till,l,t+1}),$$
(30)

where $f_{BDtill,t+1}$ is the fraction of density change of the topsoil layer after tillage, $f_{BDtill,t}$ is the density effect before tillage, $W_{sat,till,l,t+1}$ and $W_{fc,till,l,t+1}$ are adjusted moisture content at saturation and field capacity after tillage and $W_{sat,l,t}$ and $W_{fc,l,t}$ are the moisture content at saturation and field capacity before tillage.

Reconsolidation of the tilled soil layer is accounted for following the same approach by Williams et al. (2015). The rate of reconsolidation depends on the rate of infiltration and the sand content of the soil. This ensures that the porosity and BD changes caused by tillage gradually return to their initial value before tillage. Reconsolidation is calculated the following way:

386 $sz = 0.2 \cdot In \cdot \frac{1 + 2 \cdot Sa / (Sa + e^{8.597 - 0.075 \cdot Sa})}{z_{till}^{0.6}}$, (31)

387 $f = \frac{sz}{sz + e^{3.92 - 0.0226 \cdot sz}}$, (32)

388 $f_{BDtill,t+1} = f_{BDtill,t} + f \cdot (1 - f_{BDtill,t})$, (33)

389

390 where sz is the scaling factor for the tillage layer and z_{till} is the depth of the tilled layer in m. This allows for a

391 faster settling of recently tilled soils with high precipitation and for soils with a high sand content. In dry areas

392 with low precipitation and for soils with low sand content, the soil settles slower and might not consolidate back

393 to its initial state. This is accounted for by taking the previous bulk density before tillage into account. The effect

394 of tillage on BD can vary from year to year, but $f_{BDtill,t}$ cannot be below 0.667 or above 1 so that unwanted

395 amplification is not possible. We do not yet account for fluffy soil syndrome processes (i.e. when the soil does

396 not settle over time) and negative implication from this, which results in an unfavorable soil particle distribution

397 that can cause a decline in productivity (Daigh and DeJong-Hughes, 2017).

4 Model setup

4.1 Model input, initialization and spin-up

400 In order to bring vegetation patterns and SOM pools into a dynamic equilibrium stage, we make use of a 5000

401 years spin-up simulation of only natural vegetation, which recycles the first 30 years of climate input following

402 the procedures of von Bloh et al. (2018). For simulations with land-use inputs and to account for agricultural

403 management, a second spin-up of 390 years is conducted, to account for historical land-use change, which is

404 introduced in the year 1700. The spatial resolution of all input data and model simulations is 0.5°. Land use data

405 is based on crop-specific shares of MIRCA2000 (Portmann et al., 2010) and cropland and grassland time series

406 since 1700 from HYDE3 (Klein Goldewijk et al., 2010) as described by Fader et al. (2010). Per default setting,

407 intercrops are grown on all setaside stands in all simulations (Bondeau et al. 2007). As we are here interested in

408 the effects of tillage on cropland, we ignore all natural vegetation in grid cells with cropland by scaling existing

409 cropland shares to 100%. We drive the model with daily mean temperature from the Climate Research Unit

410 (CRU TS version 3.23, University of East Anglia Climate Research Unit, 2015; Harris et al., 2014), monthly

411 precipitation data from the Global Precipitation Climatology Centre (GPCC Full Data Reanalysis version 7.0;

412 Becker et al., 2013) and shortwave downward and net longwave downward radiation data from the ERA-Interim

413 data set (Dee et al., 2011). Static soil texture classes are taken from the Harmonized World Soil Database

414 (HWSD) version 1.1 (Nachtergaele et al., 2009) and aggregated to 0.5° resolution by using the dominant soil

415 type. Twelve different soil textural classes are distinguished according to the USDA soil texture classification

416 and one unproductive soil type, which is referred to as "rock and ice". Soil pH data are taken from the WISE

417 data set (Batjes, 2005). The NOAA/ESRL Mauna Loa station (Tans and Keeling, 2015) provides atmospheric

418 CO_2 concentrations. Deposition of N was taken from the ACCMIP database (Lamarque et al., 2013).

4.2 Simulation options and evaluation set-up

420 The new tillage management implementation allows for specifying different tillage and residue systems. We

421 conducted four contrasting simulations on current cropland area with or without the application of tillage and

with or without removal of residues (Table 1). The default setting for conventional tillage is: mE=0.9 and TL=0.95. In the tillage scenario, tillage is conducted twice a year, at sowing and after harvest. Soil water properties are updated on a daily basis, enabling the tillage effect to be effective from the subsequent day onwards until it wears off due to soil settling processes. The four different management settings (MS) for global simulations are as the following: 1) full tillage and residues left on the field (T_R), 2) full tillage and residues are removed (T_NR), 3) no-till and residues are retained on the field (NT_R), and 4) no-till and residues are removed from the field (NT_NR). The specific parameters for these four settings are listed in Table 1. The default MS is T_R and was introduced in the second spin-up from the year 1700 onwards, as soon as human land use is introduced in the individual grid cells (Fader et al. 2010). All of the four MS simulations were run for 109 years, starting from year 1900. Unless specified differently, the outputs of the four different MS simulations were analyzed using the relative differences between each output variable using T_R as the baseline MS;

$$RD_X = \frac{X_{MS}}{X_{T\_R}} - 1, \tag{34}$$

where RD_X is the relative difference between the management scenarios for variable X and X_{MS} and X_{T_R} are the values of variable X of the MS of interest and the baseline management systems: conventional tillage with residues left on the field (T_R). Spin-up simulations and relative differences for equation (34) were adjusted, if a different MS was used as reference system, e.g. if reference data are available for comparisons of different MS. The effects were analyzed for different time scales: the three year average of year 1 to 3 for short-term effects, the average after year 9 to 11 for mid-term effects and the average of year 19 to 21 for long-term effects. Depending on available reference data in the literature, the specific duration and default MS of the experiment were chosen. The results of the simulations are compared to literature values from selected meta-analyses. Meta-analyses allow for the comparison of globally modeled results to a set of combined results of individual studies from all around the world, assuming that the data basis presented in meta-analyses is representative. A comparison to individual site-specific studies would require detailed site-specific simulations making use of climatic records for that site and details on the specific land-use history. Results of individual site-specific experiments can differ substantially between sites, which hampers the interpretation at larger scales. We calculated the median and the 5th and 95th percentile (values within brackets) between MS in order to compare the model results to the meta-analyses, where averages and 95% confidence intervals (CI) are mostly reported. We chose medians rather than arithmetic averages to reduce outlier effects, which is especially important for relative changes that strongly depend on the baseline value. If region-specific values were reported in the meta-analyses, e.g. climate zones, we compared model results of these individual regions, following the same approach for each study, to the reported regional value ranges.

To analyze the effectiveness of selected individual processes (see Fig. 1) without confounding feedback processes, we conducted additional simulations of the four different MS on bare soil with uniform dry matter litter input (simulation NT_NR_bs and NT_R_bs1 to NT_R_bs5) of uniform composition (C:N ratio of 20), no atmospheric N deposition and static fertilizer input (Elliott et al., 2015). This helps isolating soil processes, as any feedbacks via vegetation performance is eliminated in this setting.

461   *[Table 1]*

462   **5 Evaluation and discussion**

463   **5.1 Tillage effects on hydraulic properties**

464   Table 2 presents the calculated soil hydraulic properties of tillage for each of the soil classes prior to and after

465   tillage (mE of 0.9), combined with a SOM content in the tilled soil layer of 0% and 8%. In general, both tillage

466   and a higher SOM content tend to increase whc, $W_{sat,l}$, $W_{fc,l}$ and Ks_l. Clay soils are an exception, since higher

467   SOM content decreases whc, $W_{sat,l}$ and $W_{fc,l}$, and increases Ks_l. The effect of increasing SOM content on whc,

468     $W_{sat,l}$ and $W_{fc,l}$ is greatest in the soil classes sand and loamy sand. The increasing effects of tillage on the

469   hydraulic properties are generally weaker compared to an increase in SOM by 8% (maximum SOM content for

470   computing soil hydraulic properties in the model). While tillage (mE of 0.9, 0% SOM) in sandy soils increase

471   whc by 83%, 8% of SOM can increase whc in an untilled soil by 105% and in a tilled soil by 84%. As

472   comparison in silty loam soils with 0% SOM, tillage (mE of 0.9) increases whc by 16%, while 8% SOM can

473   increase whc by 31% and by 26% for untilled and tilled soil, respectively.

474   The PTF by Saxton and Rawls (2006) uses an empirical relationship between SOM, soil texture and

475   hydraulic properties derived from the USDA soil database, implying that the PTF is likely to be more accurate

476   within the US than outside. A PTF developed for global scale application is, to our knowledge, not yet

477   developed. Nevertheless PTFs are used in a variety of global applications, despite the limitations to validate at

478   this scale (Van Looy et al., 2017).

479

480   *[Table 2]*

481   **5.2 Productivity**

482   In our simulations adopting NT_R slightly increases productivity for all rain-fed crops simulated (wheat, maize,

483   pulses, rapeseed) on average, but ranges from increases to decreases across all cropland globally. This increase

484   can be observed for the first three years (Fig. S2 in the Supplement), and for the first ten years (Fig. 2A and 2B).

485   All the results shown here and in the subsequent sections are calculated as RD following Eq. (34), unless

486   otherwise stated. The numbers discussed in this section refer to the productivity after 10 years (average of year

487   9-11). The largest positive impact can be found for rapeseed, where NT_R results in a median increase of +3.5%

488   (5th, 95th percentiles: -24.5%, +57.8%). The positive impact is lowest for maize, with median increases by +1.8%

489   (5th, 95th percentiles: -24.6%, +56.2%). The median productivity of wheat increases slightly by +2.5% (5th, 95th

490   percentiles: -15.2%, +53.5%) under NT_R. The slight increases in median productivity under NT_R are

491   contrasting to the values reported by Pittelkow et al. (2015b), who reports slight decreases in productivity for

492   wheat and maize and small median increases for rapeseed (Table 3). They report both positive and negative

493   effects for wheat and rapeseed, but only negative effects for maize. Pittelkow et al. (2015b) identify aridity and

494   crop type as the most important factors influencing the responses of productivity to the introduction of no-till

495   systems with residues left on the field. The aridity index was determined by dividing the mean annual

496   precipitation by potential evaporation. No-till performed best under rain-fed conditions in dry climates (aridity

497   index <0.65), by which the overall response was equal or positive compared to T_R.

498   The positive effects on productivity under NT_R in dry regions can also be found in our simulations. For
499   instance, wheat productivity increases substantially under NT_R whereas this effect diminishes with increases in
500   aridity indexes (Fig. 2A). Similar results are found for maize productivity (Fig. 2B). This positive effect can be
501   attributed to the presence of surface litter, which leads to higher soil moisture conservation through increased
502   water infiltration into the soil and decreases in evaporation. Areas where crop productivity is limited by soil
503   water could therefore potentially benefit from NT_R (Pittelkow et al., 2015a). The influence of climatic
504   condition of no-till effects on productivity was already found by several other studies (e.g. Ogle et al., 2012;
505   Pittelkow et al., 2015a; van Kessel et al., 2013). Ogle et al. (2012) found declines in productivity, but that these
506   declines were larger in the cooler and wetter climates. Pittelkow et al. (2015a) found only small declines in
507   productivity in dry areas, but emphasized that increases in yield can be found when no-till is combined with
508   residues and crop rotation. This was not the case for humid areas (aridity index >0.65), there declines in
509   productivity were larger under no-till regardless if residues and crop rotations were applied. Finally, van Kessel
510   et al. (2013) found declines in productivity after adapting to no-till in dry areas (-11%) and humid areas (-3%).
511   However, in their analysis it is not clear how crop residues are treated in no-till and tillage (i.e. removed or
512   retained).
513   Negative effects of NT_R on productivity can be observed in mainly the tropical areas. As soil moisture
514   increases in the tropical areas under NT_R as well (Fig. 5C), the decline is resulting from a decrease in N
515   availability is the soil (Fig. 5D). Soil moisture drives many N-related processes that can cause a decline of N. For
516   instance, the increase in soil moisture can lead to an increase in denitrification, which decreases the amount of
517   NO_3^- (which will be more discussed in chapter 5.5). On the other hand, mineralization can also be reduced if soil
518   moisture is too high. However, the soil moisture- N availability and yield feedback is complex as many
519   processes are involved.
520
521   [Fig. 2]

522   **5.3. Soil C stocks and fluxes**

523   We evaluate the effects of tillage and residue management on simulated soil C dynamics and fluxes for CO_2
524   emissions from cropland soils, relative change in C input, SOC turnover time as well as relative changes in soil
525   and litter C stocks of the topsoil (0.3 m). In our simulation CO_2 emissions initially decrease for the average of the
526   first three years by a median value of -11.9% (5th, 95th percentile: -24.1%, +2.0%) after introducing no-till
527   (NT_R vs. T_R) (Fig. S3A in the Supplement) and soil and litter C stocks increase. After ten years duration
528   (average of year 9-11) however, both CO_2 emissions and soil and litter C stocks are higher under NT_R than
529   under T_R (Fig. 3A, 3D). Median CO_2 emissions from NT_R compared to T_R increase by +1.7% (5th, 95th
530   percentile: -17.4%, +32.4%) (Fig. 3A), while at the same time median topsoil and litter C also increase by +5.3%
531   (5th, 95th percentile: +1.4%, +12.8%) (Fig. 3D), i.e. the soil and litter C stock has already increased enough to
532   sustain higher CO_2 emissions. There are two explanations for CO_2 increase in the long term: 1) more C input
533   from increased net primary production (NPP) for NT_R or 2) a higher decomposition rate over time under
534   NT_R, due to changes in e.g. soil moisture or temperature. Initially CO_2 emissions decrease almost globally due
535   to increased turnover times under T_R (Fig. S3C in the Supplement), but after ten years, CO_2 emissions start to
536   increase in drier regions, while they still decrease in most humid regions (Fig. 3A). The median of the relative

537 differences in mean residence time of soil carbon for NT_R compared to T_R is small, but variable (+0.0% after
538 ten years, 5th, 95th percentile: -22.9%, +23.7%) (Fig. 3C), and mean residence time shows similar spatial patterns,
539 i.e. it decreases in drier areas but increases in more humid areas. The drier regions are also the areas where we
540 observe a positive effect of reduced evaporation and increased infiltration on plant growth, i.e. in these regions
541 the C-input into soils is substantially increased under NT_R compared to T_R (Fig. 3B) (see also 5.2 for
542 productivity). As such, both mechanisms that affect CO_2 emissions are reinforcing each other in many regions.
543 This is in agreement with the meta-analyses conducted by Pittelkow et al. (2015b), who report a positive effect
544 on yields (and thus general productivity and thus C-input) of no-till compared to conventional tillage in dry
545 climates. Their results show that in general, no-till performs best relative to conventional tillage under water-
546 limited conditions, due to enhanced water-use efficiencies when residues are retained.

547   Abdalla et al. (2016) reviewed the effect of tillage, no-till and residues management and found that if
548 residues are returned, no-till compared to conventional tillage increases soil and litter C content by 5.0% (95th
549 CI: -1.0%, +9.2%) and decreases CO_2 emissions from soils by -23.0% (95th CI: -35.0%, -13.8%) (Table 3).
550 These findings of Abdalla et al. (2016) are in line to our findings for CO_2 emissions if we consider the first three
551 years of duration for CO_2 emissions and ten years duration for topsoil and litter C. Abdalla et al. (2016) do not
552 explicitly specify a time of duration for these results. If we only analyze the tillage effect without taking residues
553 into account (T_NR vs. NT_NR), we find in our simulation that topsoil and litter C decreases by -18.0% (5th,
554 95th percentile: -42.5%, -0.5%) after twenty years, while CO_2 emissions increase by +21.3% (5th, 95th percentile:
555 -1.1%, +125.2%) mostly in humid regions, whereas they start increasing in drier regions (Table 3). Abdalla et al.
556 (2016) also reported soil and litter C changes from a T_NR vs. NT_NR comparison and reported a decrease in
557 soil and litter C under T_NR of -12.0% (95th CI: -15.3%, -5.1%) and a CO_2 increase of +18.0% (95th CI: +9.4%,
558 +27.3%), which is well in line with our model results.

559   Ogle et al. (2005) conducted a meta-analysis and reported SOC changes from NT_R compared to T_R
560 system with medium C input, grouped for different climatic zones. They found a +23%, +17%, + 16% and +10%
561 mean increase in SOC after converting from a conventional tillage to a no-till system for more than 20 years for
562 tropical moist, tropical dry, temperate moist and temperate dry climates, respectively. We only find a +4.8%,
563 +8.3%, +3.5% and +5.8% mean increase in topsoil and litter C for these regions, respectively. However, Ogle et
564 al. (2005) analyzed the data by comparing a no-till system with high C inputs from rotation and residues to a
565 conventional tillage system with medium C input from rotation and residues. We compare two similarly
566 productive systems with each other, where residues are either left on the field or incorporated through tillage
567 (NT_R vs. T_R), which may explain why we see smaller relative effects in the simulations. Comparing a high
568 input system with a medium or a low input system will essentially lead to an amplification of soil and litter C
569 changes over time; nevertheless we are still able to generally reproduce a SOC increase over longer periods.

570   Unfortunately there are high discrepancies in the literature with regard to no-till effects on soil and litter C,
571 since the high increases found by Ogle et al. (2005) are not supported by the findings of Abdalla et al. (2016).
572 Ranaivoson et al. (2017) found that crop residues left on the field increases soil and litter C content, which is in
573 agreement with our simulation results.

574

575 *[Fig. 3]*

5.4 Water fluxes

We evaluate the effects of tillage and residue management on water fluxes by analyzing soil evaporation and surface runoff. Our results show that evaporation and surface runoff under NT_R compared to T_R are generally reduced by -44.3% (5th, 95th percentiles: -64.5, -17.4%) and by -57.8% (5th, 95th percentiles: -74.6%, -26.1%), respectively (Fig. S4A and S4B in the Supplement). We also analyzed soil evaporation and surface runoff for different amounts of surface litter loads and cover on bare soil without vegetation in order to compare our results to literature estimates from field experiments. We find that both the reduction in evaporation and surface runoff are dependent on the residue load, which translates into different rates of surface litter cover.

On the process side, water fluxes highly influence plant productivity and are affected by tillage and residue management (Fig. 1). Surface litter, which is left on the surface of the soil, creates a barrier that reduces evaporation and also increases the rate of infiltration into the soil. Litter which is incorporated into the soil through tillage loses this function to cover the soil. Both, the reduction of soil evaporation and the increase of rainfall infiltration contribute to increased soil moisture and hence plant water availability. The model accounts for both processes. Scopel et al. (2004) modeled the effect of maize residues on soil evaporation calibrated from two tropical sites and found that a presence of 100 g m^{-2} surface litter decrease soil evaporation by -10% to -15% in the data, whereas our model shows a median decrease in evaporation of -6.6% (5th, 95th percentiles: -26.1%, +20.3%) globally (Fig. S5A in the Supplement). The effect of a higher amount of surface litter is much more dominate, as Scopel et al. (2004) found that 600 g m^{-2} surface litter reduced evaporation by approx. -50%. For the same litter load our model shows a median decrease in evaporation by -72.6% (5th, 95th percentiles: -81.5%, -49.1%) (Fig. S5B in the Supplement), which is higher than the results found by Scopel et al. (2004). We further analyze and compare our model results to the meta-analysis from Ranaivoson et al. (2017), who reviewed the effect of surface litter on evaporation and surface runoff and other agro-ecological functions. Ranaivoson et al. (2017) and the studies compiled by them not explicitly distinguish between the different compartments of runoff (e.g. lateral-, surface-runoff). We assume that they measured surface runoff, since lateral runoff is difficult to measure and has to be considered in relation to plot size. In Fig. 4, modeled global results for relative evaporation and surface runoff change for 10, 30, 50, 70 and 90% soil cover on bare soil are compared to literature values from Ranaivoson et al. (2017). Concerning the effect of soil cover on evaporation (Fig. 4A), we find that we are well in line with literature estimates from Ranaivoson et al. (2017) for up to 70% soil cover, especially when analyzing humid climates. For higher soil cover ≥70%, the model seems to be more in line with literature values for arid regions. Overall for high soil cover of 90%, the model seems to overestimate the reduction of evaporation. It should be noted that the estimates from Ranaivoson et al. (2017) are only taken from two field studies, which are only representative for the local climatic and soil conditions, since global data on the effect of surface litter on evaporation are not available. The general effect of surface litter on the reduction in soil evaporation is thus captured by the model, but the model seems to overestimate the response at high litter loads. It is not entirely clear from the literature if these experiments have been carried on bare soil without vegetation. If crops are also grown in the experiments, water can be used for transpiration which is otherwise available for evaporation, which could explain why the model overestimates the effect of surface litter on evaporation on bare soil without any vegetation.

Ranaivoson et al. (2017) also investigated the runoff reduction under soil cover, but the results do not show a clear picture. In theory, surface litter reduces surface runoff and literature generally supports this assumption (Kurothe et al., 2014; Wilson et al., 2008), but the magnitude of the effect varies. Fig. 4B compares our modeled

617   results under different soil cover to the literature values from Ranaivoson et al. (2017). This shows that modeled

618   results across all global cropland are on the upper end of the effect of surface runoff reduction from soil cover,

619   but they are still well within the range reported by Ranaivoson et al. (2017). The amount of water which is

620   infiltrated (and thus not going into surface runoff) is affected by the parameter p in Eq. (11), which is dependent

621   on the amount of surface litter cover (f_{surf}). The parameterization of p is chosen to be at the upper end of the

622   approach by Jägermeyr et al. (2016) at full surface litter cover, as this should substantially reduce surface runoff

623   (Tapia-Vargas et al., 2001) and thus increase infiltration rates (Strudley et al., 2008). The parametrization of p

624   can be adjusted if better site-specific information on slope, soils crusting and rainfall intensity is available.

625

626   *[Fig. 4]*

627   **5.5 N$_2$O fluxes**

628   Switching from tillage to no-till management with leaving residues on the fields (NT_R vs. T_R) increases N$_2$O

629   emissions by a median of +20.8% (5th, 95th percentile: -3.6%, +325.5%) (Fig. S6A in the Supplement). The

630   strongest increase is found in the cool temperate zone where the average increase is +23.5% (5th, 95th percentile:

631   -0.1%, +664.4%) (Fig. S6E in the Supplement). The lowest increase is found in the tropical zone +15.8% (5th,

632   95th percentile: -7.3%, +72.1%) (Fig. S6C in the Supplement).

633   The increase in N$_2$O emissions after switching to no-till is in agreement with several literature studies (Linn

634   and Doran, 1984; Mei et al., 2018; van Kessel et al., 2013; Zhao et al., 2016) (Table 3). Mei et al. (2018) reports

635   an overall increase of +17.3% (95th CI: +4.6%, +31.1%), which is in agreement with our median estimate.

636   However, the regional patterns over the different climatic regimes are in less agreement. LPJmL simulations

637   strongly underestimate the increase in N$_2$O emissions in the tropical zone, whereas simulations overestimate the

638   response in cool temperate and humid zones and to some extent in the warm temperate zone (Table 3).

639   In general, N$_2$O emissions are formed in two separate processes: nitrification and denitrification. The increase

640   in N$_2$O emissions after adapting to NT_R is mainly resulting from denitrification in our simulations (+55.9%,

641   Fig. 5A). This increase is visible in most of the regions. The N$_2$O emissions resulting from nitrification decrease

642   mostly (median of -6.0%, Fig. 5B) but tends to increase in dry areas. The increase in denitrification and decrease

643   in nitrification, results in a decrease in NO$_3^-$ (median of -26.4%), which appears to be stronger in the tropical

644   areas as well (Fig. 5D). The transformation of mineral N to N$_2$O is not only affected by the nitrification and

645   denitrification rates, but also by substrate availability (NH$_4^+$ and NO$_3^-$). These in turn are affected by nitrification

646   and denitrification rates, but also by other processes, such as plant uptake and leaching. In the Sahel zone for

647   example, denitrification decreases and nitrification increases, but NO$_3^-$ stocks decline, because leaching increase

648   more strongly (Fig. S7 in the Supplement).

649   In LPJmL, denitrification and nitrification rates are mainly driven by soil moisture and to a lesser extent by

650   soil temperature, soil C (denitrification) and soil pH (nitrification). A strong increase in annually averaged soil

651   moisture can be observed after adapting NT_R (median of +18.9%, Fig. 5C). Denitrification, as an anoxic

652   process, increases non-linearly beyond a soil moisture threshold (von Bloh et al. 2018), whereas there is an

653   optimum soil moisture for nitrification, which is reduced at low and high soil moisture content. In wet regions,

654   as in the tropical and humid areas, nitrification is thus reduced by no-till practices whereas it increases in dryer

655   regions. The increase in soil moisture under NT_R is caused by higher water infiltration rates and reduced soil

656 evaporation (see section 5.4). Also, no-till practices tend to increase bulk density and thus higher relative soil

657 moisture contents (Fig. 1) also affecting nitrification and denitrification rates and therefore N_2O emissions (van

658 Kessel et al., 2013; Linn and Doran, 1984).

659   Empirical evidence shows that the introduction of no-till practices on N_2O emissions can cause both

660 increases and decreases in N_2O emissions (van Kessel et al., 2013). This variation in response is not surprising,

661 as tillage affects several biophysical factors that influence N_2O emissions (Fig. 1) in possibly contrasting

662 manners (van Kessel et al., 2013; Snyder et al., 2009). For instance no-till can lower soil temperature exchange

663 between soil and atmosphere, through the presence of litter residues, which can reduce N_2O emissions (Enrique

664 et al. 1999). Reduced N_2O emissions under no-till compared to tillage MS can also be observed in the model

665 results, for instance in Northern Europe and areas in Brazil (Fig. S6A in the Supplement).

666   As several biophysical factors are affected, N_2O emissions are characterized by significant spatial and

667 temporal variability. As a result, the estimation of N_2O emissions are accompanied with high uncertainties

668 (Butterbach-Bahl et al., 2013), which hampers the evaluation of the model results (Chatskikh et al., 2008;

669 Mangalassery et al., 2015).

670   The deviations from the model results compared to the meta-analyses especially for specific climatic regimes

671 (i.e. tropical- and cool temperate) require further investigations and verification, including model simulations for

672 specific sites at which experiments have been conducted. The sensitivity of N_2O emissions highlights the

673 importance of correctly simulating soil moisture. However, simulating soil moisture is subject to strong feedback

674 with vegetation performance and comes with uncertainties, as addressed by e.g. Seneviratne et al. (2010). The

675 effects of different management settings (as conducted here), on N_2O emissions and soil moisture requires

676 therefore further analyses, ideally in different climate regimes, soil types and in combination with other

677 management settings (e.g. N-fertilizers). We expect that further studies using this tillage implementation in

678 LPJmL will increase the understanding of management effects on soil nitrogen dynamics. The great diversity in

679 observed responses in N_2O emissions to management options (Mei et al. 2018) renders modeling these effects as

680 challenging, but we trust that the ability of LPJmL5.0-tillage to represent the different components can also help

681 to better understand their interaction under different environmental conditions.

682

683 *[Fig. 5]*

684

685 *[Table 3]*

686 **5.6 General discussion**

687 The implementation of tillage into the global ecosystem model LPJmL opens opportunities to assess the effects

688 of different tillage practices on agricultural productivity and its environmental impacts, such as nutrient cycles,

689 water consumption, GHG emissions and C sequestration and is a general model improvement to the previous

690 version of LPJmL (von Bloh et al., 2018). The implementation involved 1) the introduction of a surface litter

691 pool that is incorporated into the soil column at tillage events and the subsequent effects on soil evaporation and

692 infiltration, 2) dynamically accounting for SOM content in computing soil hydraulic properties, and 3)

693 simulating tillage effects on bulk density and the subsequent effects of changed soil water properties and all

694 water-dependent processes (Fig. 1).

In general, a global model implementation on tillage practices is difficult to evaluate, as effects are reported often to be quite variable, depending on local soil and climatic conditions. The model results were evaluated with data compiled from meta-analyses, which implies several limitations. Due to the limited amount of available meta-analyses, not all fluxes and stocks could be evaluated within the different management scenarios. For the evaluation we focused on productivity, soil and litter C stocks and fluxes, water fluxes and N_2O dynamics. The sample size in some of these meta-analyses was sometimes low, which may result in biases if not a representative set of climate and soil combinations was tested. Clearly a comparison of a small sample size to simulations of the global cropland is challenging. Nevertheless, the meta-analyses gave the best overview of the overall effects of tillage practices that have been reported for various individual experiments.

We find that the model results for NT_R compared to T_R are generally in agreement with literature with regard to magnitude and direction of the effects on C stocks and fluxes. Despite some disagreement between reported ranges in effects and model simulations, we find that the diversity in modeled responses across environmental gradients is an asset of the model. The underlying model mechanisms, as the initial decrease in CO_2 emissions after introduction of no-till practices that can be maintained for longer time periods in moist regions, but is inverted in dry regions due to the feedback of higher water availability on plant productivity and reduced turnover times and generally increasing soil carbon stocks (Fig. 3), are plausible and in line with general process understanding. Certainly, the interaction of the different processes may not be captured correctly and further research on this is needed. We trust that this model implementation representing this complexity allows for further research in this direction. For water fluxes, the model seems to overestimate the effect of surface residue cover on evaporation for high surface cover, but the evaluation is also constrained by the small number of suitable field studies. Effects can also change over time so that a comparison needs to consider the timing, history and duration of management changes and specific local climatic and soil conditions. The overall effect of NT_R compared to T_R on N_2O emissions are in agreement with literature as well. However, the regional patterns over the different climatic regimes are in less agreement. N_2O emissions are highly variable in space and time and are very sensitive to soil water dynamics (Butterbach-Bahl et al., 2013). The simulation of soil water dynamics differs per soil type as the calculation of the hydraulic parameters is texture specific. Moreover, these parameters are now changed after a tillage event. The effects of tillage on N_2O emissions, as well as other processes that are driven by soil water (e.g. CO_2, water dynamics) can therefore be different per soil type. The soil specific effects of tillage on N_2O and CO_2 emissions was already studied by Abdalla et al. (2016) and Mei et al. (2018). Abdalla et al. (2016) found that differences in CO_2 emissions between tilled and untilled soils are largest in sandy soils (+29%), whereas the differences in clayey soils are much smaller (+12%). Mei et al. (2018) found that clay content <20% significantly increases N_2O emissions (+42.9%) after adapting to conservation tillage, whereas this effect for clay content >20% is smaller (+2.9%). These studies show that soil type-specific tillage effects on several processes can be of importance and should be investigated in more detail in future studies. The interaction of all relevant processes is complex, as seen in Fig. 1, which can also lead to high uncertainties in the model. Again, we think that this model implementation captures substantial aspects of this complexity and thus lays the foundation for further research.

It is important to note that not all processes related to tillage and no-till are taken into account in the current model implementation. For instance, NT_R can improve soil structure (e.g., aggregates) due to increased faunal activity (Martins et al., 2009), which can result in a decrease in BD. Although tillage can have several advantages for the farmer, e.g. residue incorporation and topsoil loosening, it can also have several

736 disadvantages. For instance, tillage can cause compaction of the subsoil (Bertolino et al., 2010), which result in
737 an increase in BD (Podder et al., 2012) and creates a barrier for percolating water, leading to ponding and an
738 oversaturated topsoil. Strudley et al. (2008) however observed diverging effects of tillage and no-till on
739 hydraulic properties, such as BD, Ks and whc for different locations. They argue that affected processes of
740 agricultural management have complex coupled effects on soil hydraulic properties, as well as that variations in
741 space and time often lead to higher differences than the measured differences between the management
742 treatments. They also argue that characteristics of soil type and climate are unique for each location, which
743 cannot simply be transferred from one field location to another. A process-based representation of tillage effects
744 as in this extension of LPJmL allows for further studying management effects across diverse environmental
745 conditions, but also to refine model parameters and implementations where experimental evidence suggests
746 disagreement.

747 One of the primary reasons for tillage, weed control, is also not accounted for in LPJmL5.0-tillage or in other
748 ecosystem models. As such, different tillage and residue management strategies can only be assessed with
749 respect to their biogeochemical effects, but only partly with respect to their effects on productivity and not with
750 respect to some environmental effects (e.g. pesticide use). Our model simulations show that crop yields increase
751 under no-till practices in dry areas but decrease in wetter regions (Fig. 2). However, the median response is
752 positive, which may be in part because the water saving effects from increased soil cover with residues are
753 overestimated or because detrimental effects, such as competition with weeds, are not accounted for.

754 The included processes now allow us to analyze long term feedbacks of productivity on soil and litter C
755 stocks and N dynamics. Nevertheless the results need to be interpreted carefully, due to the capacity of the model
756 and implemented processes. We also find that the modeled impacts of tillage are very diverse in space as a result
757 of different framing conditions (soil, climate, management) and feedback mechanisms, such as improved
758 productivity in dry areas if residue cover increases plant available water. The process-based representation in the
759 LPJmL5.0-tillage of tillage and residue management and the effects on water fluxes such as evaporation and
760 infiltration at the global scale is unique in the context of global biophysical models (e.g. Friend et al. 2014,
761 LeQuéré et al., 2018). Future research on improved parameterization and the implementation of more detailed
762 representation of tillage processes and the effects on soil water processes, changes in porosity and subsoil
763 compaction, effects on biodiversity and on soil N dynamics is needed in order to better assess the impacts of
764 tillage and residue management at the global scale. The spatial resolution needed to resolve processes, such as
765 erosion, data availability, and model structure need to be considered in further model development (Lutz et al.
766 2019). As such, some processes, such as a detailed representation of soil crusting processes, may remain out of
767 reach for global-scale modeling.

768 **6 Conclusion**

769 We described the implementation of tillage related processes into the global ecosystem model LPJmL5.0-tillage.
770 The extended model was tested under different management scenarios and evaluated by comparing to reported
771 impact ranges from meta-analyses on C, water and N dynamics as well as on crop yields.

772 We find that mostly arid regions benefit from a no-till management with leaving residues on the field, due to
773 the water saving effects of surface litter. We are able to broadly reproduce reported tillage effects on global
774 stocks and fluxes, as well as regional patterns of these changes, with LPJmL5.0-tillage, but deviations in N-

775 fluxes need to be further examined. Not all effects of tillage, including one of its primary reasons, weed control,
776 could not be accounted for in this implementation. Uncertainties mainly arise because of the multiple feedback
777 mechanisms affecting the overall response to tillage, especially as most processes are affected by soil moisture.
778 The processes and feedbacks presented in this implementation are complex and evaluation of effects is often
779 limited in the availability of reference data. Nonetheless, the implementation of more detailed tillage-related
780 mechanics into global ecosystem model LPJmL improves our ability to represent different agricultural systems
781 and to understand management options for climate change adaptation, agricultural mitigation of GHG emissions
782 and sustainable intensification. We trust that this model implementation and the publication of the underlying
783 source code promote research on the role of tillage for agricultural production, its environmental impact and
784 global biogeochemical cycles.
785

786 *Code and data availability.*The source code is publicly available under the GNU AGPL version 3 license. An
787 exact version of the source code described here is archived under https://doi.org/10.5281/zenodo.2652136.
788

789 *Author contributions.* F.L and T.H. both share the lead authorship for this manuscript. They had equal input in
790 designing and conducting the model implementation, model runs, analysis and writing of the manuscript. S.R.
791 contributed to simulation analysis and manuscript preparation/evaluation. J.H. contributed to the code
792 implementation, evaluation and analysis and edited the paper. S.S. contributed to the code implementation and
793 evaluation and edited the paper. W.v.B. contributed to the code implementation and evaluation and edited the
794 paper. J.S. contributed to the study design and edited the paper. C.M. contributed to the study design, supervised
795 implementation, simulations and analyses and edited the paper.
796

797 *Competing interests.* All authors declare no competing interests.
798

799 *Acknowledgements*
800 F.L., T.H. and S.R. gratefully acknowledge the German Ministry for Education and Research (BMBF) for
801 funding this work, which is part of the MACMIT project (01LN1317A). J.H. acknowledges BMBF funding
802 through the SUSTAg project (031B0170A). We thank the two anonymous reviewers for their helpful comments
803 on earlier versions of the paper.

804

805 **References**

806 Abdalla, K., Chivenge, P., Ciais, P. and Chaplot, V.: No-tillage lessens soil CO_2 emissions the most under arid
807 and sandy soil conditions: results from a meta-analysis, Biogeosciences, 13(12), 3619–3633, doi:10.5194/bg-
808 13-3619-2016, 2016.

809 Armand, R., Bockstaller, C., Auzet, A.-V. and Van Dijk, P.: Runoff generation related to intra-field soil surface
810 characteristics variability: Application to conservation tillage context, Soil Tillage Res., 102(1), 27–37,
811 doi:https://doi.org/10.1016/j.still.2008.07.009, 2009.

812 Aslam, T., Choudhary, M. A. and Saggar, S.: Influence of land-use management on CO_2 emissions from a silt
813 loam soil in New Zealand, Agric. Ecosyst. Environ., 77(3), 257–262, doi:10.1016/S0167-8809(99)00102-4,
814 2000.

815 Balland, V., Pollacco, J. A. P. and Arp, P. A.: Modeling soil hydraulic properties for a wide range of soil
816 conditions, Ecol. Model., 219(3–4), 300–316, doi:10.1016/j.ecolmodel.2008.07.009, 2008.

817 Batjes, N.: ISRIC-WISE global data set of derived soil properties on a 0.5 by 0.5 degree grid (version 3.0),
818 ISRIC – World Soil Information, Wageningen., 2005.

819 Becker, A., Finger, P., Meyer-Christoffer, A., Rudolf, B., Schamm, K., Schneider, U. and Ziese, M.: A
820 description of the global land-surface precipitation data products of the Global Precipitation Climatology
821 Centre with sample applications including centennial (trend) analysis from 1901–present, Earth Syst. Sci.
822 Data, 5(1), 71–99, doi:https://doi.org/10.5194/essd-5-71-2013, 2013.

823 Bertolino, A. V. F. A., Fernandes, N. F., Miranda, J. P. L., Souza, A. P., Lopes, M. R. S. and Palmieri, F.:
824 Effects of plough pan development on surface hydrology and on soil physical properties in Southeastern
825 Brazilian plateau, J. Hydrol., 393(1), 94–104, doi:10.1016/j.jhydrol.2010.07.038, 2010.

826 Best, M. J., Pryor, M., Clark, D. B., Rooney, G. G., Essery, R., Ménard, C. B., Edwards, J. M., Hendry, M. A.,
827 Porson, A. and Gedney, N.: The Joint UK Land Environment Simulator (JULES), model description–Part 1:
828 energy and water fluxes, Geosci. Model Dev., 4(3), 677–699, 2011.

829 von Bloh, W., Schaphoff, S., Müller, C., Rolinski, S., Waha, K. and Zaehle, S.: Implementing the nitrogen cycle
830 into the dynamic global vegetation, hydrology, and crop growth model LPJmL (version 5.0), Geosci. Model
831 Dev., 11(7), 2789–2812, doi:https://doi.org/10.5194/gmd-11-2789-2018, 2018.

832 Bondeau, A., Smith, P. C., Zaehle, S., Schaphoff, S., Lucht, W., Cramer, W., Gerten, D., Lotze-Campen, H.,
833 MüLler, C., Reichstein, M. and Smith, B.: Modelling the role of agriculture for the 20th century global
834 terrestrial carbon balance, Glob. Change Biol., 13(3), 679–706, doi:10.1111/j.1365-2486.2006.01305.x,
835 2007.

836 Brady, N. C. and Weil, R. R.: The nature and properties of soils, Pearson Prentice Hall Upper Saddle River.,
837 2008.

838 Butterbach-Bahl, K., Baggs, E. M., Dannenmann, M., Kiese, R. and Zechmeister-Boltenstern, S.: Nitrous oxide
839 emissions from soils: how well do we understand the processes and their controls?, Philos. Trans. R. Soc. B
840 Biol. Sci., 368(1621), 20130122, 2013.

841 Chatskikh, D., Olesen, J. E., Hansen, E. M., Elsgaard, L. and Petersen, B. M.: Effects of reduced tillage on net
842 greenhouse gas fluxes from loamy sand soil under winter crops in Denmark, Agric. Ecosyst. Environ.,
843 128(1–2), 117–126, doi:10.1016/j.agee.2008.05.010, 2008.

844 Chen, H., Hou, R., Gong, Y., Li, H., Fan, M. and Kuzyakov, Y.: Effects of 11 years of conservation tillage on
845 soil organic matter fractions in wheat monoculture in Loess Plateau of China, Soil Tillage Res., 106(1), 85–
846 94, doi:10.1016/j.still.2009.09.009, 2009.

847 Ciais, P., Gervois, S., Vuichard, N., Piao, S. L. and Viovy, N.: Effects of land use change and management on
848 the European cropland carbon balance, Glob. Change Biol., 17(1), 320–338, doi:10.1111/j.1365-
849 2486.2010.02341.x, 2011.

850 Clark, D. B., Mercado, L. M., Sitch, S., Jones, C. D., Gedney, N., Best, M. J., Pryor, M., Rooney, G. G., Essery,
851   R. L. H. and Blyth, E.: The Joint UK Land Environment Simulator (JULES), model description–Part 2:
852   carbon fluxes and vegetation dynamics, Geosci. Model Dev., 4(3), 701–722, 2011.

853 Cosby, B. J., Hornberger, G. M., Clapp, R. B. and Ginn, T. R.: A Statistical Exploration of the Relationships of
854   Soil Moisture Characteristics to the Physical Properties of Soils, Water Resour. Res., 20(6), 682–690,
855   doi:10.1029/WR020i006p00682, 1984.

856 Daigh, A. L. M. and DeJong-Hughes, J.: Fluffy soil syndrome: When tilled soil does not settle, J. Soil Water
857   Conserv., 72(1), 10A-14A, doi:10.2489/jswc.72.1.10A, 2017.

858 Dee, D. P., Uppala, S. M., Simmons, A. J., Berrisford, P., Poli, P., Kobayashi, S., Andrae, U., Balmaseda, M. A.,
859   Balsamo, G., Bauer, P., Bechtold, P., Beljaars, A. C. M., Berg, L. van de, Bidlot, J., Bormann, N., Delsol, C.,
860   Dragani, R., Fuentes, M., Geer, A. J., Haimberger, L., Healy, S. B., Hersbach, H., Hólm, E. V., Isaksen, L.,
861   Kållberg, P., Köhler, M., Matricardi, M., McNally, A. P., Monge-Sanz, B. M., Morcrette, J.-J., Park, B.-K.,
862   Peubey, C., Rosnay, P. de, Tavolato, C., Thépaut, J.-N. and Vitart, F.: The ERA-Interim reanalysis:
863   configuration and performance of the data assimilation system, Q. J. R. Meteorol. Soc., 137(656), 553–597,
864   doi:10.1002/qj.828, 2011.

865 Elliott, J., Müller, C., Deryng, D., Chryssanthacopoulos, J., Boote, K. J., Büchner, M., Foster, I., Glotter, M.,
866   Heinke, J., Iizumi, T., Izaurralde, R. C., Mueller, N. D., Ray, D. K., Rosenzweig, C., Ruane, A. C. and
867   Sheffield, J.: The Global Gridded Crop Model Intercomparison: data and modeling protocols for Phase 1
868   (v1.0), Geosci. Model Dev., 8(2), 261–277, doi:10.5194/gmd-8-261-2015, 2015.

869 Enrique, G. S., Braud, I., Jean-Louis, T., Michel, V., Pierre, B. and Jean-Christophe, C.: Modelling heat and
870   water exchanges of fallow land covered with plant-residue mulch, Agric. For. Meteorol., 97(3), 151–169,
871   doi:10.1016/S0168-1923(99)00081-7, 1999.

872 Fader, M., Rost, S., Müller, C., Bondeau, A. and Gerten, D.: Virtual water content of temperate cereals and
873   maize: Present and potential future patterns, J. Hydrol., 384(3–4), 218–231,
874   doi:10.1016/j.jhydrol.2009.12.011, 2010.

875 Friend, A. D., Lucht, W., Rademacher, T. T., Keribin, R., Betts, R., Cadule, P., Ciais, P., Clark, D. B., Dankers,
876   R., Falloon, P. D., Ito, A., Kahana, R., Kleidon, A., Lomas, M. R., Nishina, K., Ostberg, S., Pavlick, R.,
877   Peylin, P., Schaphoff, S., Vuichard, N., Warszawski, L., Wiltshire, A. and Woodward, F. I.: Carbon
878   residence time dominates uncertainty in terrestrial vegetation responses to future climate and atmospheric
879   CO2, Proc. Natl. Acad. Sci., 111(9), 3280–3285, doi:10.1073/pnas.1222477110, 2014.

880 Glab, T. and Kulig, B.: Effect of mulch and tillage system on soil porosity under wheat (Triticum aestivum), Soil
881   Tillage Res., 99(2), 169–178, doi:https://doi.org/10.1016/j.still.2008.02.004, 2008.

882 Govers, G., Vandaele, K., Desmet, P., Poesen, J. and Bunte, K.: The role of tillage in soil redistribution on
883   hillslopes, Eur. J. Soil Sci., 45(4), 469–478, 1994.

884 Green, T. R., Ahuja, L. R. and Benjamin, J. G.: Advances and challenges in predicting agricultural management
885   effects on soil hydraulic properties, Geoderma, 116(1–2), 3–27, doi:10.1016/S0016-7061(03)00091-0, 2003.

886 Gregory, J. M.: Soil cover prediction with various amounts and types of crop residue, Trans. ASAE, 25(5),
887   1333–1337, doi:10.13031/2013.33723, 1982.

888 Guérif, J., Richard, G., Dürr, C., Machet, J. M., Recous, S. and Roger-Estrade, J.: A review of tillage effects on
889   crop residue management, seedbed conditions and seedling establishment, Soil Tillage Res., 61(1–2), 13–32,
890   2001.

891 Harris, I., Jones, P. D., Osborn, T. J. and Lister, D. H.: Updated high-resolution grids of monthly climatic
892   observations – the CRU TS3.10 Dataset, Int. J. Climatol., 34(3), 623–642, doi:10.1002/joc.3711, 2014.

893 Hillel, D.: Chapter 12 Soil temperature and heat flow, in Introduction to Envrionental Soil Physics, pp. 215–
894   234, Elsevier Academic Press Inc, Amsterdam., 2004.

895 Holland, J. M.: The environmental consequences of adopting conservation tillage in Europe: reviewing the
896   evidence, Agric. Ecosyst. Environ., 103(1), 1–25, 2004.

897 Horton, R., Horn, R., Bachmann, J. and Peth, S.: Essential Soil Physics - An introduction to soil processes,
898   functions, structure and mechanic, E. Schweizerbart'sche Verlagsbuchhandlung., 2016.

899 Jägermeyr, J., Gerten, D., Heinke, J., Schaphoff, S., Kummu, M. and Lucht, W.: Water savings potentials of
900   irrigation systems: global simulation of processes and linkages, Hydrol. Earth Syst. Sci., 19(7), 3073, 2015.

901 Jägermeyr, J., Gerten, D., Schaphoff, S., Heinke, J., Lucht, W. and Rockström, J.: Integrated crop water
902   management might sustainably halve the global food gap, Environ. Res. Lett., 11(2), 025002,
903   doi:10.1088/1748-9326/11/2/025002, 2016.

904 Jarvis, P. G. and McNaughton, K. G.: Stomatal control of transpiration: scaling up from leaf to region, Adv.
905   Ecol. Res., 15, 1–49, doi:10.1016/S0065-2504(08)60119-1, 1986.

906 van Kessel, C., Venterea, R., Six, J., Adviento-Borbe, M. A., Linquist, B. and Van Groenigen, K. J.: Climate,
907   duration, and N placement determine N2O emissions in reduced tillage systems: a meta-analysis, Glob.
908   Change Biol., 19(1), 33–44, 2013.

909 Klein Goldewijk, K., Beusen, A., Van Drecht, G. and De Vos, M.: The HYDE 3.1 spatially explicit database of
910   human-induced global land-use change over the past 12,000 years: HYDE 3.1 Holocene land use, Glob.
911   Ecol. Biogeogr., 20(1), 73–86, doi:10.1111/j.1466-8238.2010.00587.x, 2010.

912 Kurothe, R. S., Kumar, G., Singh, R., Singh, H. B., Tiwari, S. P., Vishwakarma, A. K., Sena, D. R. and Pande,
913   V. C.: Effect of tillage and cropping systems on runoff, soil loss and crop yields under semiarid rainfed
914   agriculture in India, Soil Tillage Res., 140, 126–134, doi:10.1016/j.still.2014.03.005, 2014.

915 Lal, R.: Managing soil water to improve rainfed agriculture in India, J. Sustain. Agric., 32(1), 51–75, 2008.

916 Lamarque, J.-F., Dentener, F., McConnell, J., Ro, C.-U., Shaw, M., Vet, R., Bergmann, D., Cameron-Smith, P.,
917   Dalsoren, S., Doherty, R., Faluvegi, G., Ghan, S. J., Josse, B., Lee, Y. H., MacKenzie, I. A., Plummer, D.,
918   Shindell, D. T., Skeie, R. B., Stevenson, D. S., Strode, S., Zeng, G., Curran, M., Dahl-Jensen, D., Das, S.,
919   Fritzsche, D. and Nolan, M.: Multi-model mean nitrogen and sulfur deposition from the Atmospheric
920   Chemistry and Climate Model Intercomparison Project (ACCMIP): evaluation of historical and projected
921   future changes, Atmospheric Chem. Phys., 13(16), 7997–8018, doi:https://doi.org/10.5194/acp-13-7997-
922   2013, 2013.

923 LeQuéré, C., Andrew, R. M., Friedlingstein, P., Sitch, S., Pongratz, J., Manning, A. C., Korsbakken, J. I., Peters,
924   G. P., Canadell, J. G., Jackson, R. B., Boden, T. A., Tans, P. P., Andrews, O. D., Arora, V. K., Bakker, D. C.
925   E., Barbero, L., Becker, M., Betts, R. A., Bopp, L., Chevallier, F., Chini, L. P., Ciais, P., Cosca, C. E., Cross,
926   J., Currie, K., Gasser, T., Harris, I., Hauck, J., Haverd, V., Houghton, R. A., Hunt, C. W., Hurtt, G., Ilyina,
927   T., Jain, A. K., Kato, E., Kautz, M., Keeling, R. F., Klein Goldewijk, K., Körtzinger, A., Landschützer, P.,
928   Lefèvre, N., Lenton, A., Lienert, S., Lima, I., Lombardozzi, D., Metzl, N., Millero, F., Monteiro, P. M. S.,
929   Munro, D. R., Nabel, J. E. M. S., Nakaoka, S., Nojiri, Y., Padin, X. A., Peregon, A., Pfeil, B., Pierrot, D.,
930   Poulter, B., Rehder, G., Reimer, J., Rödenbeck, C., Schwinger, J., Séférian, R., Skjelvan, I., Stocker, B. D.,
931   Tian, H., Tilbrook, B., Tubiello, F. N., Laan-Luijkx, I. T. van der, Werf, G. R. van der, Heuven, S. van,
932   Viovy, N., Vuichard, N., Walker, A. P., Watson, A. J., Wiltshire, A. J., Zaehle, S. and Zhu, D.: Global
933   Carbon Budget 2017, Earth Syst. Sci. Data, 10(1), 405–448, doi:https://doi.org/10.5194/essd-10-405-2018,
934   2018.

935 Levis, S., Hartman, M. D. and Bonan, G. B.: The Community Land Model underestimates land-use CO 2
936   emissions by neglecting soil disturbance from cultivation, Geosci. Model Dev., 7(2), 613–620, 2014.

937 Linn, D. M. and Doran, J. W.: Effect of water-filled pore space on carbon dioxide and nitrous oxide production
938   in tilled and nontilled soils 1, Soil Sci. Soc. Am. J., 48(6), 1267–1272, 1984.

939 Lugato, E., Leip, A. and Jones, A.: Mitigation Potential of Soil Carbon Management Overestimated by
940   Neglecting N2O Emissions, Nat. Clim. Change, 8(3), 219, 2018.

941 Lutz, F., Stoorvogel, J. J. and Müller, C.: Options to model the effects of tillage on N2O emissions at the global
942   scale, Ecol. Model., 392, 212–225, 2019.

943 Maharjan, G. R., Prescher, A.-K., Nendel, C., Ewert, F., Mboh, C. M., Gaiser, T. and Seidel, S. J.: Approaches to
944   model the impact of tillage implements on soil physical and nutrient properties in different agro-ecosystem
945   models, Soil Tillage Res., 180, 210–221, 2018.

946 Mangalassery, S., Sjoegersten, S., Sparkes, D. L. and Mooney, S. J.: Examining the potential for climate change
947   mitigation from zero tillage, J. Agric. Sci., 153(7), 1151–1173, doi:10.1017/S0021859614001002, 2015.

948 Martins, I. C. F., Cividanes, F. J., Barbosa, J. C., Araújo, E. de S. and Haddad, G. Q.: Faunal analysis and
949   population fluctuation of Carabidae and Staphylinidae (Coleoptera) in no-tillage and conventional tillage
950   systems, Rev. Bras. Entomol., 53(3), 432–443, 2009.

951 Mauser, W. and Bach, H.: PROMET–Large scale distributed hydrological modelling to study the impact of
952   climate change on the water flows of mountain watersheds, J. Hydrol., 376(3–4), 362–377, 2009.

953 Mei, K., Wang, Z., Huang, H., Zhang, C., Shang, X., Dahlgren, R. A., Zhang, M. and Xia, F.: Stimulation of N 2
954   O emission by conservation tillage management in agricultural lands: A meta-analysis, Soil Tillage Res.,
955   182, 86–93, doi:10.1016/j.still.2018.05.006, 2018.

956 Minasny, B. and McBratney, A. B.: Limited effect of organic matter on soil available water capacity, Eur. J. Soil
957   Sci., 69(1), 39–47, 2018.

958 Nachtergaele, F., Van Velthuizen, H., Verelst, L., Batjes, N., Dijkshoorn, K., van Engelen, V., Fischer, G.,
959   Jones, A., Montanarella, L. and Petri, M.: Harmonized World Soil Database (version 1.1). Food and
960   Agriculture Organization of the United Nations. Rome, Italy and IIASA, Laxenburg, Austria., [online]
961   Available from: http://www.fao.org/soils-portal/soil-survey/soil-maps-and-databases/harmonized-world-soil-
962   database-v12/en/ (Accessed 12 July 2018), 2009.

963 Ogle, S. M., Breidt, F. J. and Paustian, K.: Agricultural management impacts on soil organic carbon storage
964   under moist and dry climatic conditions of temperate and tropical regions, Biogeochemistry, 72(1), 87–121,
965   doi:10.1007/s10533-004-0360-2, 2005.

966 Ogle, S. M., Swan, A. and Paustian, K.: No-till management impacts on crop productivity, carbon input and soil
967   carbon sequestration, Agric. Ecosyst. Environ., 149, 37–49, doi:10.1016/j.agee.2011.12.010, 2012.

968 Oleson, K. W., Lawrence, D. M., Gordon, B., Flanner, M. G., Kluzek, E., Peter, J., Levis, S., Swenson, S. C.,
969   Thornton, E. and Feddema, J.: Technical description of version 4.0 of the Community Land Model (CLM),
970   2010.

971 Olin, S., Lindeskog, M., Pugh, T. a. M., Schurgers, G., Wårlind, D., Mishurov, M., Zaehle, S., Stocker, B. D.,
972   Smith, B. and Arneth, A.: Soil carbon management in large-scale Earth system modelling: implications for
973   crop yields and nitrogen leaching, Earth Syst. Dyn., 6(2), 745–768, doi:https://doi.org/10.5194/esd-6-745-
974   2015, 2015.

975 Oorts, K., Merckx, R., Gréhan, E., Labreuche, J. and Nicolardot, B.: Determinants of annual fluxes of CO2 and
976   N2O in long-term no-tillage and conventional tillage systems in northern France, Soil Tillage Res., 95(1),
977   133–148, doi:10.1016/j.still.2006.12.002, 2007.

978 Pittelkow, C. M., Liang, X., Linquist, B. A., van Groenigen, K. J., Lee, J., Lundy, M. E., van Gestel, N., Six, J.,
979   Venterea, R. T. and van Kessel, C.: Productivity limits and potentials of the principles of conservation
980   agriculture, Nature, 517(7534), 365–368, doi:10.1038/nature13809, 2015a.

981 Pittelkow, C. M., Linquist, B. A., Lundy, M. E., Liang, X., van Groenigen, K. J., Lee, J., van Gestel, N., Six, J.,
982   Venterea, R. T. and van Kessel, C.: When does no-till yield more? A global meta-analysis, Field Crops Res.,
983   183, 156–168, doi:10.1016/j.fcr.2015.07.020, 2015b.

984 Podder, M., Akter, M., Saifullah, A. and Roy, S.: Impacts of Plough Pan on Physical and Chemical Properties of
985   Soil, J. Environ. Sci. Nat. Resour., 5(1), doi:10.3329/jesnr.v5i1.11594, 2012.

986 Portmann, F. T., Siebert, S. and Döll, P.: MIRCA2000—Global monthly irrigated and rainfed crop areas around
987   the year 2000: A new high-resolution data set for agricultural and hydrological modeling, Glob. Biogeochem.
988   Cycles, 24(1), GB1011, doi:10.1029/2008GB003435, 2010.

989 Pribyl, D. W.: A critical review of the conventional SOC to SOM conversion factor, Geoderma, 156(3–4), 75–
990   83, doi:10.1016/j.geoderma.2010.02.003, 2010.

991 Priestley, C. H. B. and Taylor, R. J.: On the assessment of surface heat flux and evaporation using large-scale
992   parameters, Mon. Weather Rev., 100(2), 81–92, 1972.

993 Pugh, T. A. M., Arneth, A., Olin, S., Ahlström, A., Bayer, A. D., Klein Goldewijk, K., Lindeskog, M. and
994   Schurgers, G.: Simulated carbon emissions from land-use change are substantially enhanced by accounting
995   for agricultural management, Environ. Res. Lett., 10(12), 124008, doi:10.1088/1748-9326/10/12/124008,
996   2015.

997 Ranaivoson, L., Naudin, K., Ripoche, A., Affholder, F., Rabeharisoa, L. and Corbeels, M.: Agro-ecological
998   functions of crop residues under conservation agriculture. A review, Agron. Sustain. Dev., 37(26), 1–17,
999   doi:10.1007/s13593-017-0432-z, 2017.

1000 Saxton, K. E. and Rawls, W. J.: Soil Water Characteristic Estimates by Texture and Organic Matter for
1001   Hydrologic Solutions, Soil Sci. Soc. Am. J., 70(5), 1569–1577, doi:10.2136/sssaj2005.0117, 2006.

1002 Schaphoff, S., Heyder, U., Ostberg, S., Gerten, D., Heinke, J. and Lucht, W.: Contribution of permafrost soils to
1003   the global carbon budget, Environ. Res. Lett., 8(1), 014026, doi:10.1088/1748-9326/8/1/014026, 2013.

1004 Schaphoff, S., Forkel, M., Müller, C., Knauer, J., Bloh, W. von, Gerten, D., Jägermeyr, J., Lucht, W., Rammig,
1005   A., Thonicke, K. and Waha, K.: LPJmL4 – a dynamic global vegetation model with managed land – Part 2:
1006   Model evaluation, Geosci. Model Dev., 11(4), 1377–1403, doi:https://doi.org/10.5194/gmd-11-1377-2018,
1007   2018a.

1008 Schaphoff, S., von Bloh, W., Rammig, A., Thonicke, K., Biemans, H., Forkel, M., Gerten, D., Heinke, J.,
1009   Jägermeyr, J., Knauer, J., Langerwisch, F., Lucht, W., Müller, C., Rolinski, S. and Waha, K.: LPJmL4 – a
1010   dynamic global vegetation model with managed land – Part 1: Model description, Geosci Model Dev, 11(4),
1011   1343–1375, doi:10.5194/gmd-11-1343-2018, 2018b.

1012 Scopel, E., Da Silva, F. A. M., Corbeels, M., Affholder, F. and Maraux, F.: Modelling crop residue mulching
1013   effects on water use and production of maize under semi-arid and humid tropical conditions, Agronomie,
1014   24(6–7), 383–395, doi:10.1051/agro:2004029, 2004.

1015 Seneviratne, S. I., Corti, T., Davin, E. L., Hirschi, M., Jaeger, E. B., Lehner, I., Orlowsky, B. and Teuling, A. J.:
1016   Investigating soil moisture–climate interactions in a changing climate: A review, Earth-Sci. Rev., 99(3–4),
1017   125–161, 2010.

1018 Sitch, S., Smith, B., Prentice, I. C., Arneth, A., Bondeau, A., Cramer, W., Kaplan, J. O., Levis, S., Lucht, W.,
1019   Sykes, M. T. and others: Evaluation of ecosystem dynamics, plant geography and terrestrial carbon cycling in
1020   the LPJ dynamic global vegetation model, Glob. Change Biol., 9(2), 161–185, doi:10.1046/j.1365-
1021   2486.2003.00569.x, 2003.

1022 Six, J., Ogle, S. M., Jay breidt, F., Conant, R. T., Mosier, A. R. and Paustian, K.: The potential to mitigate global
1023   warming with no-tillage management is only realized when practised in the long term, Glob. Change Biol.,
1024   10(2), 155–160, doi:10.1111/j.1529-8817.2003.00730.x, 2004.

1025 Smith, P., Martino, D., Cai, Z., Gwary, D., Janzen, H., Kumar, P., McCarl, B., Ogle, S., O'Mara, F., Rice, C.,
1026   Scholes, B., Sirotenko, O., Howden, M., McAllister, T., Pan, G., Romanenkov, V., Schneider, U.,
1027   Towprayoon, S., Wattenbach, M. and Smith, J.: Greenhouse gas mitigation in agriculture, Philos. Trans. R.
1028   Soc. B Biol. Sci., 363(1492), 789–813, doi:10.1098/rstb.2007.2184, 2008.

1029 Snyder, C. S., Bruulsema, T. W., Jensen, T. L. and Fixen, P. E.: Review of greenhouse gas emissions from crop
1030   production systems and fertilizer management effects, Agric. Ecosyst. Environ., 133(3–4), 247–266,
1031   doi:10.1016/j.agee.2009.04.021, 2009.

1032   Steinbach, H. S. and Alvarez, R.: Changes in soil organic carbon contents and nitrous oxide emissions after
1033   introduction of no-till in Pampean agroecosystems, J. Environ. Qual., 35(1), 3–13, 2006.

1034   Strudley, M. W., Green, T. R. and Ascough, J. C.: Tillage effects on soil hydraulic properties in space and time:
1035   State of the science, Soil Tillage Res., 99(1), 4–48, doi:10.1016/j.still.2008.01.007, 2008.

1036   Tans, P. and Keeling, R.: Trends in Atmospheric Carbon Dioxide, National Oceanic & Atmospheric
1037   Administration, Earth System Research Laboratory (NOAA/ESRL), available at:
1038   https://www.esrl.noaa.gov/gmd/ccgg/trends/, [online] Available from:
1039   https://www.esrl.noaa.gov/gmd/ccgg/trends/ (Accessed 12 July 2018), 2015.

1040   Tapia-Vargas, M., Tiscareño-López, M., Stone, J. J., Oropeza-Mota, J. L. and Velázquez-Valle, M.: Tillage
1041   system effects on runoff and sediment yield in hillslope agriculture, Field Crops Res., 69(2), 173–182,
1042   doi:10.1016/S0378-4290(00)00139-8, 2001.

1043   Tian, H., Chen, G., Liu, M., Zhang, C., Sun, G., Lu, C., Xu, X., Ren, W., Pan, S. and Chappelka, A.: Model
1044   estimates of net primary productivity, evapotranspiration, and water use efficiency in the terrestrial
1045   ecosystems of the southern United States during 1895–2007, For. Ecol. Manag., 259(7), 1311–1327, 2010.

1046   Van Genuchten, M.: A Closed-form Equation for Predicting the Hydraulic Conductivity of Unsaturated Soils1,
1047   Soil Sci. Soc. Am. J., 44, doi:10.2136/sssaj1980.03615995004400050002x, 1980.

1048   Van Looy, K., Bouma, J., Herbst, M., Koestel, J., Minasny, B., Mishra, U., Montzka, C., Nemes, A., Pachepsky,
1049   Y. A., Padarian, J., Schaap, M. G., Tóth, B., Verhoef, A., Vanderborght, J., van der Ploeg, M. J.,
1050   Weihermüller, L., Zacharias, S., Zhang, Y. and Vereecken, H.: Pedotransfer Functions in Earth System
1051   Science: Challenges and Perspectives: PTFs in Earth system science perspective, Rev. Geophys., 55(4),
1052   1199–1256, doi:10.1002/2017RG000581, 2017.

1053   Vereecken, H., Weynants, M., Javaux, M., Pachepsky, Y., Schaap, M. G. and Genuchten, M. Th. van: Using
1054   Pedotransfer Functions to Estimate the van Genuchten–Mualem Soil Hydraulic Properties: A Review,
1055   Vadose Zone J., 9(4), 795, doi:10.2136/vzj2010.0045, 2010.

1056   Vereecken, H., Schnepf, A., Hopmans, J. W., Javaux, M., Or, D., Roose, T., Vanderborght, J., Young, M. H.,
1057   Amelung, W., Aitkenhead, M., Allison, S. D., Assouline, S., Baveye, P., Berli, M., Brüggemann, N., Finke,
1058   P., Flury, M., Gaiser, T., Govers, G., Ghezzehei, T., Hallett, P., Hendricks Franssen, H. J., Heppell, J., Horn,
1059   R., Huisman, J. A., Jacques, D., Jonard, F., Kollet, S., Lafolie, F., Lamorski, K., Leitner, D., McBratney, A.,
1060   Minasny, B., Montzka, C., Nowak, W., Pachepsky, Y., Padarian, J., Romano, N., Roth, K., Rothfuss, Y.,
1061   Rowe, E. C., Schwen, A., Šimůnek, J., Tiktak, A., Van Dam, J., van der Zee, S. E. a. T. M., Vogel, H. J.,
1062   Vrugt, J. A., Wöhling, T. and Young, I. M.: Modeling Soil Processes: Review, Key Challenges, and New
1063   Perspectives, Vadose Zone J., 15(5), doi:10.2136/vzj2015.09.0131, 2016.

1064   White, J. W., Jones, J. W., Porter, C., McMaster, G. S. and Sommer, R.: Issues of spatial and temporal scale in
1065   modeling the effects of field operations on soil properties, Oper. Res., 10(3), 279–299, doi:10.1007/s12351-
1066   009-0067-1, 2010.

1067   Willekens, K., Vandecasteele, B., Buchan, D. and De Neve, S.: Soil quality is positively affected by reduced
1068   tillage and compost in an intensive vegetable cropping system, Appl. Soil Ecol., 82, 61–71,
1069   doi:10.1016/j.apsoil.2014.05.009, 2014.

1070   Williams, J. R., Renard, K. G. and Dyke, P. T.: EPIC: A new method for assessing erosion's effect on soil
1071   productivity, J. Soil Water Conserv., 38(5), 381–383, 1983.

1072   Williams, J. R., Izaurralde, R. C., Williams, C. and Steglich, E. M.: Agricultural Policy / Environmental
1073   eXtender Model. Theoretical Documentation. Version 0806. AgriLIFE Research. Texas A&M System.,
1074   2015.

1075   Wilson, G. V., McGregor, K. C. and Boykin, D.: Residue impacts on runoff and soil erosion for different corn
1076   plant populations, Soil Tillage Res., 99(2), 300–307, doi:10.1016/j.still.2008.04.001, 2008.

1077   Wösten, J. H. M., Lilly, A., Nemes, A. and Le Bas, C.: Development and use of a database of hydraulic
1078   properties of European soils, Geoderma, 90(3–4), 169–185, doi:10.1016/S0016-7061(98)00132-3, 1999.

1079 Zhao, X., Liu, S.-L., Pu, C., Zhang, X.-Q., Xue, J.-F., Zhang, R., Wang, Y.-Q., Lal, R., Zhang, H.-L. and Chen,
1080   F.: Methane and nitrous oxide emissions under no-till farming in China: a meta-analysis, Glob. Change Biol.,
1081   22(4), 1372–1384, 2016.

Table 1: LPJmL simulation settings and tillage parameters used in the stylized simulations for model evaluation.

Scenario	Simulation abbreviation	Retained residue fraction on field	Tillage efficiency (TLFrac)	Mixing efficiency of tillage (mE)	Litter cover[+] (%)	Litter amount (dry matter g m^2)
Tillage + residues on 100% scaled cropland	T_R	1	0.95	0.9	variable*	variable*
Tillage + no residues on 100% scaled cropland	T_NR	0.1	0.95	0.9	variable*	variable*
No-till + residues on 100% scaled cropland	NT_R	1	0	0	variable*	variable*
No-till + no residues on 100% scaled cropland	NT_NR	0.1	0	0	variable*	variable*
No-till + no residues on bare soil	NT_NR_bs	0	0	0	0	0
No-till + residues on bare soil (1)	NT_R_bs1	1	0	0	10	17
No-till + residues on bare soil (2)	NT_R_bs2	1	0	0	30	60
No-till + residues on bare soil (3)	NT_R_bs3	1	0	0	50	117
No-till + residues on bare soil (4)	NT_R_bs4	1	0	0	70	202
No-till + residues on bare soil (5)	NT_R_bs5	1	0	0	90	383

[+]Litter cover is calculated following Gregory (1982).

*Litter amounts and litter cover are modeled internally.

Table 2: Percentage values for each soil textural class of silt, sand and clay content used in LPJmL and correspondent hydraulic parameters before and after tillage with 0% and 8% SOM using the Saxton and Rawls (2006) pedotransfer function.

Soil class	Silt (%)	Sand (%)	Clay (%)	pre-tillage, 0% SOM**				pre-tillage, 8% SOM				after tillage[++], 0% SOM				after tillage[++], 8% SOM			
				whc[++]	W_{sat}	W_{fc}	Ks	whc	W_{sat}	W_{fc}	Ks	whc	W_{sat}	W_{fc}	Ks	whc	W_{sat}	W_{fc}	Ks
Sand	5	92	3	0.04	0.42	0.05	152.05	0.09	0.71	0.19	361.98	0.08	0.59	0.09	343.67	0.14	0.80	0.21	498.92
Loamy sand	12	82	6	0.06	0.40	0.09	83.23	0.12	0.70	0.23	244.20	0.10	0.58	0.13	230.13	0.17	0.79	0.25	360.89
Sandy loam	32	58	10	0.12	0.40	0.17	32.03	0.18	0.70	0.31	152.75	0.15	0.58	0.21	125.75	0.23	0.79	0.33	239.93
Loam	39	43	18	0.15	0.41	0.26	10.69	0.21	0.69	0.37	80.46	0.19	0.59	0.30	64.76	0.25	0.78	0.39	143.99
Silty loam	70	17	13	0.22	0.42	0.31	5.49	0.29	0.75	0.42	99.77	0.26	0.59	0.34	48.23	0.32	0.83	0.44	155.38
Sandy clay loam	15	58	27	0.12	0.42	0.28	6.60	0.17	0.63	0.38	36.33	0.16	0.59	0.32	48.79	0.21	0.74	0.40	87.40
Clay loam	34	32	34	0.17	0.47	0.38	2.29	0.20	0.65	0.43	24.96	0.21	0.63	0.41	26.22	0.23	0.75	0.45	63.73
Silty clay loam	56	10	34	0.21	0.50	0.42	1.93	0.23	0.69	0.45	34.54	0.24	0.65	0.45	22.45	0.25	0.78	0.47	73.85
Sandy clay	6	52	42	0.15	0.47	0.40	0.72	0.16	0.58	0.44	5.64	0.18	0.63	0.44	16.73	0.20	0.70	0.47	29.30
Silty clay loam	47	6	47	0.20	0.56	0.48	1.64	0.18	0.65	0.46	18.69	0.23	0.69	0.50	16.67	0.20	0.76	0.48	50.99
Clay	20	22	58	0.19	0.58	0.53	0.39	0.14	0.58	0.48	2.87	0.21	0.71	0.55	8.62	0.16	0.71	0.50	20.03
Rock*	0	99	1	0.00	0.01	0.01	0.10	0.00	0.01	0.01	0.10	0.00	0.01	0.01	0.10	0.00	0.01	0.01	0.10

*Soil class rock is not affected by SOM changes and tillage practices

**For SOM we only consider the C part in SOM in gC/m^2

[+]Tillage with a *mE* of 0.9 for conventional tillage

[++]whc is calculated as: whc = W_{fc} - W_{pwp} in all cases

Table 3: Comparison of simulated model output and literature values from meta-analysis. Values for modeled results are calculated according to Eq. (34) with adjusted default management.

Variable/Scenario	Soil depth (m)	# of paired treatments	Literature mean (95% interval)	Time horizon (years)	Modeled response (median %)	Modeled response (5% and 95% percentile)	Reference
notill residue - till residue							
SOM (0.3m)	0 - 0.3	101	+5.0 (+1.0, +9.2)*‡	10§	+5.3	+1.4, +12.8	Abdalla et al., 2016
CO2		113	-23.0 (-35.0, -13.8)*	**	-11.9	-24.1, +2.0	Abdalla et al., 2016
N2O		98	+17.3 (+4.6, +31.1)*	**	+20.8	-3.6, +325.5	Mei et al., 2018
N2O (tropical)		123	+74.1 (+34.8, +119.9)†‡	**	+15.8	-7.3, +72.1	Mei et al., 2018
N2O (warm temperate)		62	+17.0 (+6.5, +29.9)†‡	**	+23.2	+6.0, +182.3	Mei et al., 2018
N2O (cool temperate)		27	-1.7 (-10.5, +8.4)†‡	**	+23.5	-0.1, +664.4	Mei et al., 2018
N2O (arid)		56	+35.0 (+7.5, +69.0)*	**	+21.1	-1.8, +496.3	Kessel et al., 2013
N2O (humid)		183	-1.5 (-11.6, +11.1)*	**	+20.7	-9.1, +63.8	Kessel et al., 2013
Yield (wheat)		47	-2.6 (-8.2, +3.8)*	10§	+2.5	-15.2, +53.5	Pittelkow et al. 2015b
Yield (maize)		64	-7.6 (-10.1, -4.3)*	10§	+1.8	-24.6, +56.2	Pittelkow et al. 2015b
Yield (rapeseed)		10	+0.7 (-2.8, +4.1)*	10§	+3.5	-24.5, +57.8	Pittelkow et al. 2015b
till noresidue - notill noresidue							
SOM (0.3m)	0 - 0.3	46	-12.0 (-15.3, -5.1)*	20§	-18.0	-42.5, -0.5	Abdalla et al., 2016
CO2		46	+18.0 (+9.4, +27.3)*	20§	+21.3	-1.1, +125.2	Abdalla et al., 2016
Yield (wheat) B		8	+2.7 (-6.3, +12.7)*	10§	-5.9	-15.7, +3.7	Pittelkow at al. 2015b
Yield (maize) B		12	-25.4 (-14.7, -34.1)*	10§	-5.0	-27.3, +12.0	Pittelkow et al. 2015b
till noresidues - till residue							
N2O		105	+1.3 (-5.4, +8.2)*‡	**	-9.7	-22.0, +3.6	Mei et al., 2018

*estimated from graph
**Time horizon of the study is unclear in the meta-analysis. The average over the first three years of model results is taken.

† includes conservation till

†† at least 30% on soil
‡ Residue management for conventional till unsure
§ Time horizon not explicitly mentioned by author
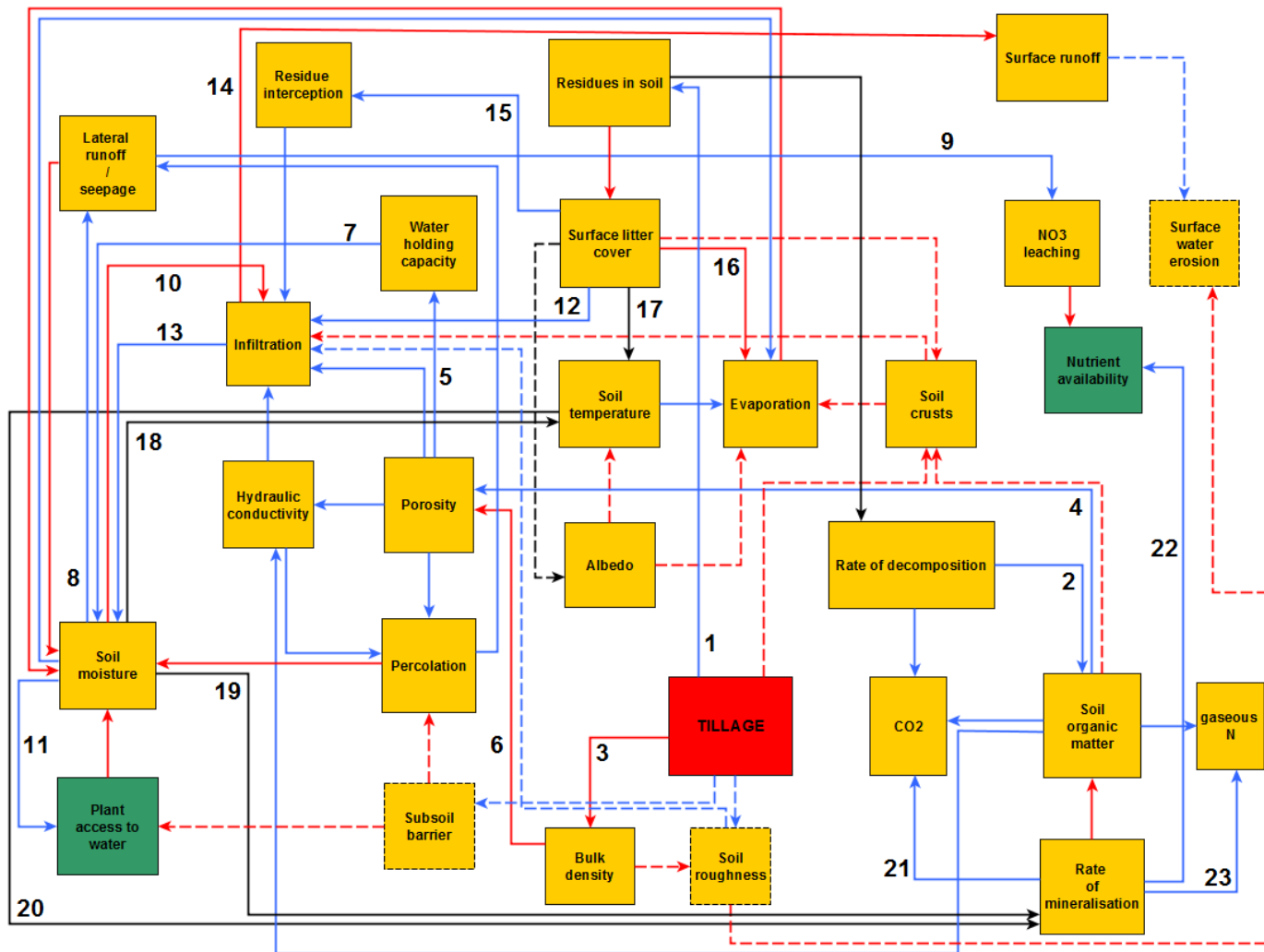
Figure 1: Flow chart diagram of feedback processes caused by tillage, which are considered (solid lines) and not considered (dashed lines) in this implementation in LPJmL5.0-tillage. Blue lines highlight positive feedbacks, red negative and black are ambiguous feedbacks. The numbers in the figure indicate the processes described in chapter 2.
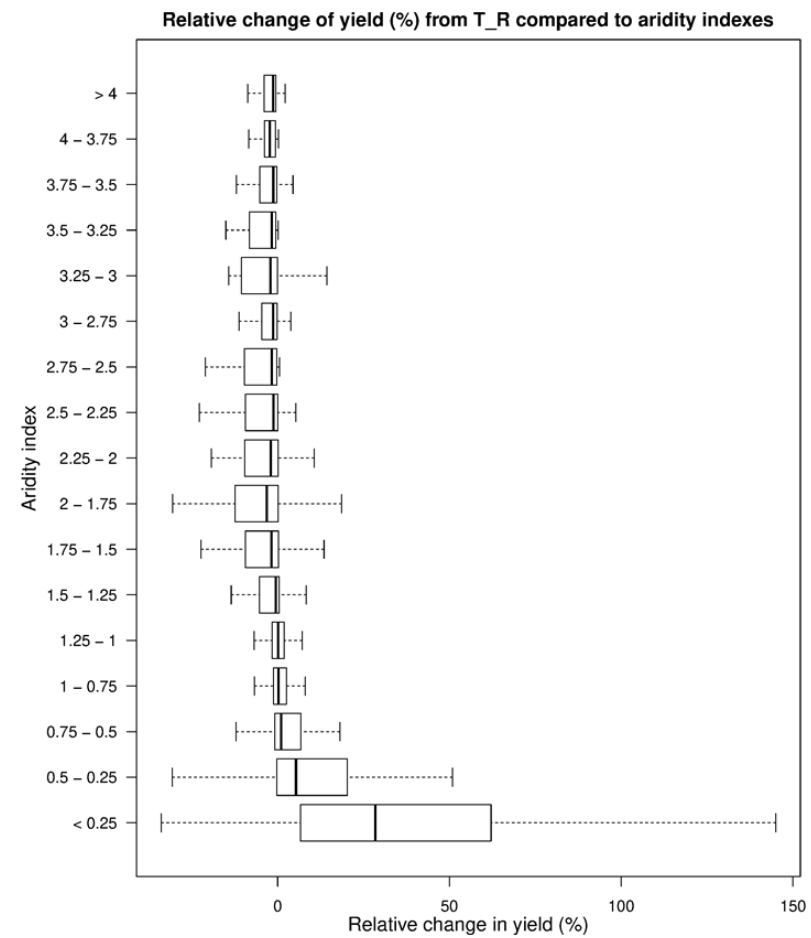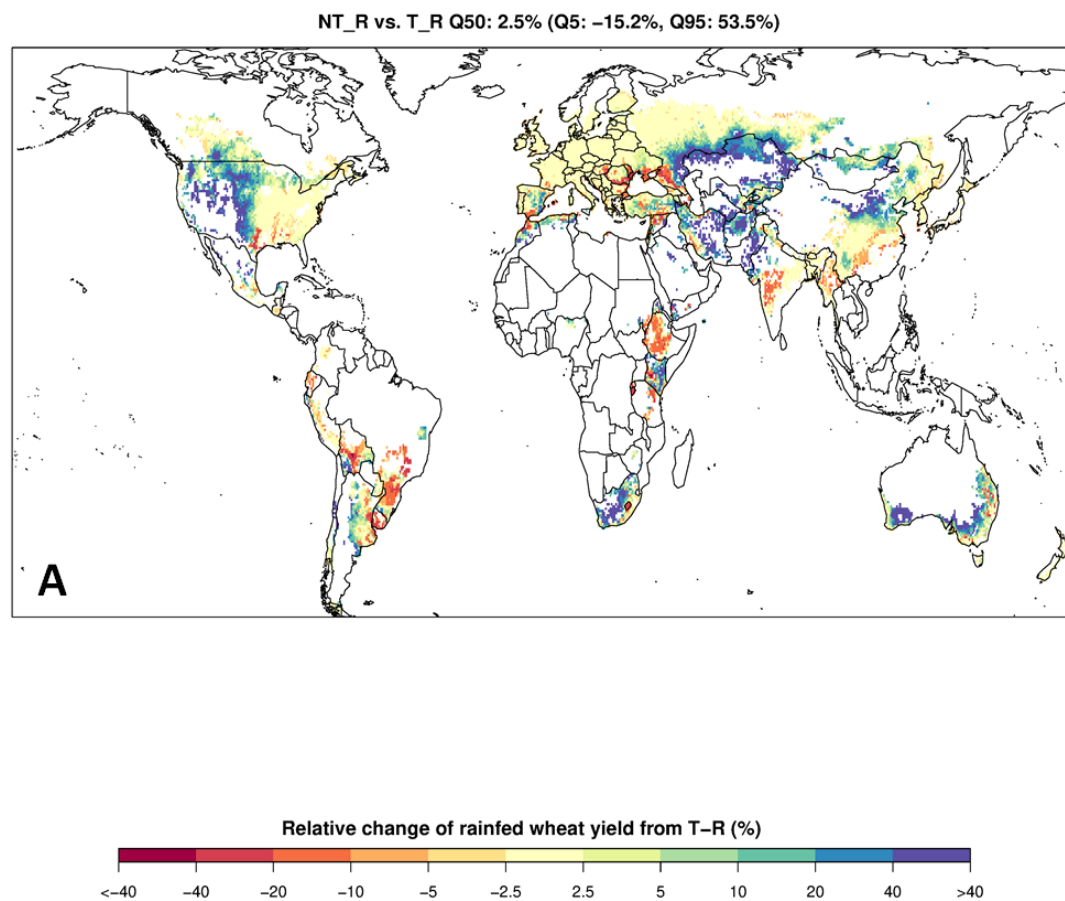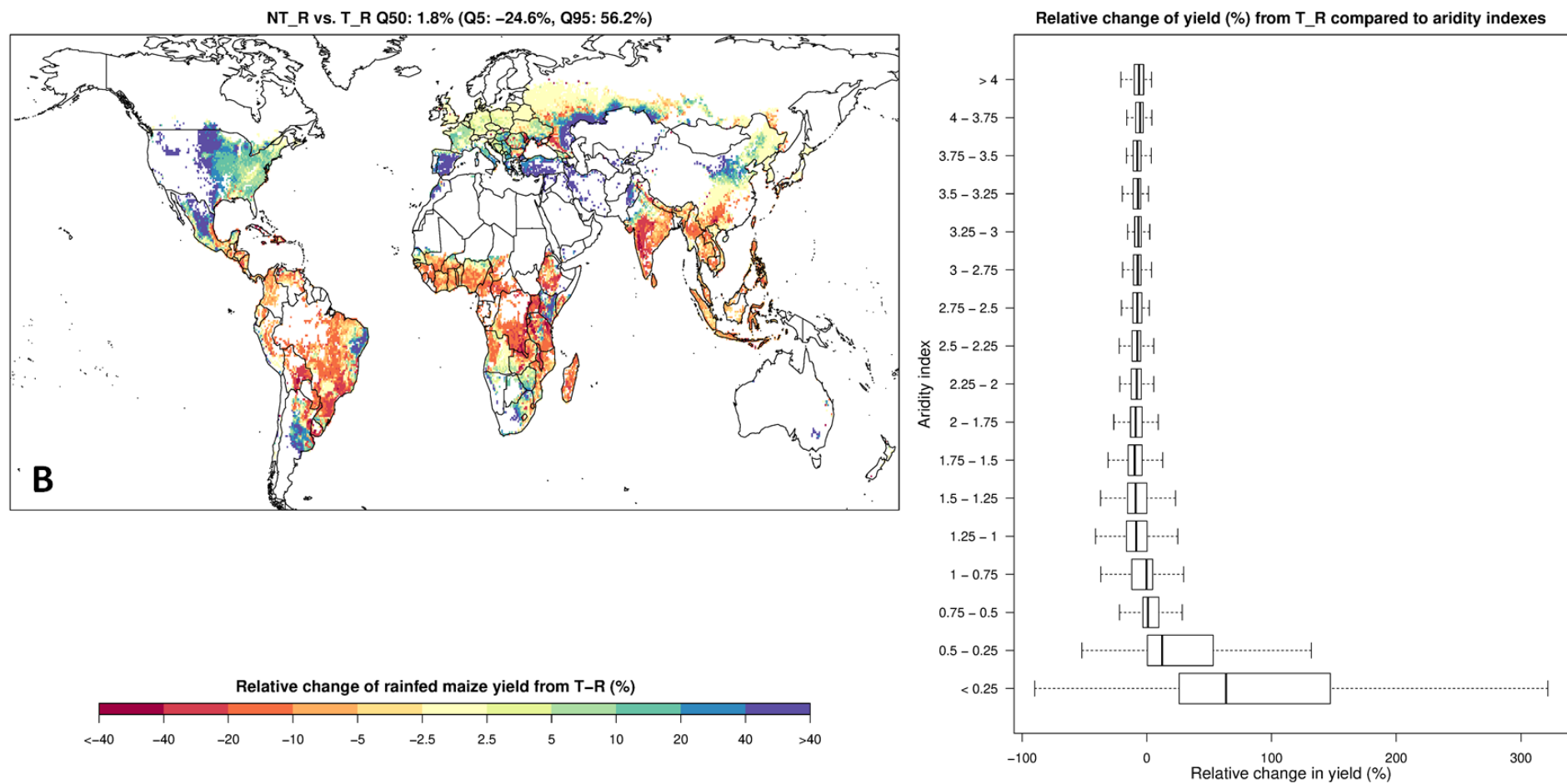
Figure 2: Relative yield changes for rain-fed wheat (A) and rain-fed maize (B) compared to aridity indexes after ten years NT_R vs. T_R. Low aridity index values indicate arid conditions as the index is defined as mean annual precipitation divided by potential evapotranspiration, following Pittelkow et al. (2015a). Substantial increases in crop yields only occur in arid regions, with aridity indices <0.75.
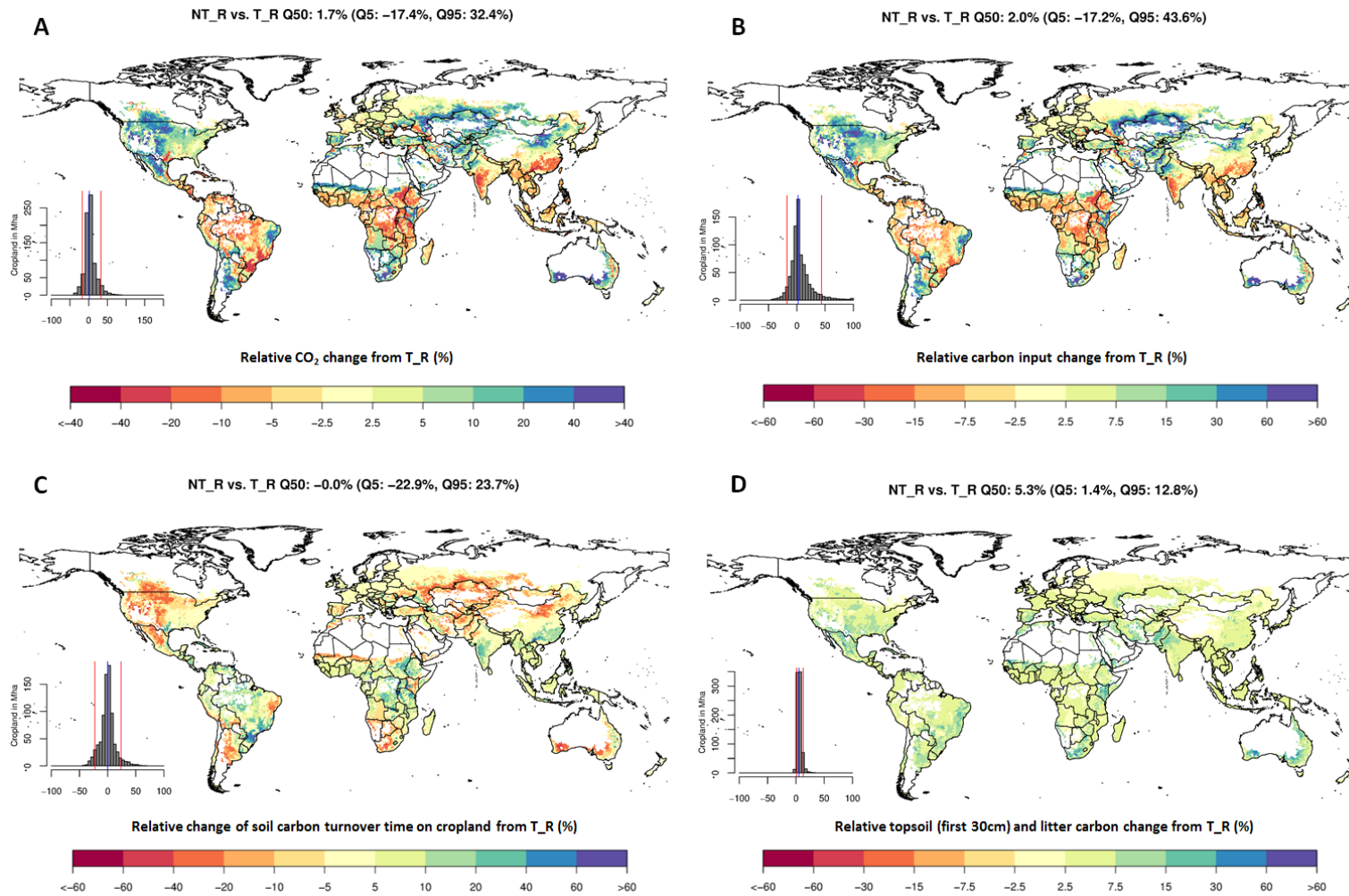
Figure 3: Relative C dynamics for NT_R vs. T_R comparison after ten years of simulation experiment (average of year 9-11) for relative CO_2 change (A), relative C input change (B), relative change of soil C turnover time (C), relative topsoil and litter C change (D).
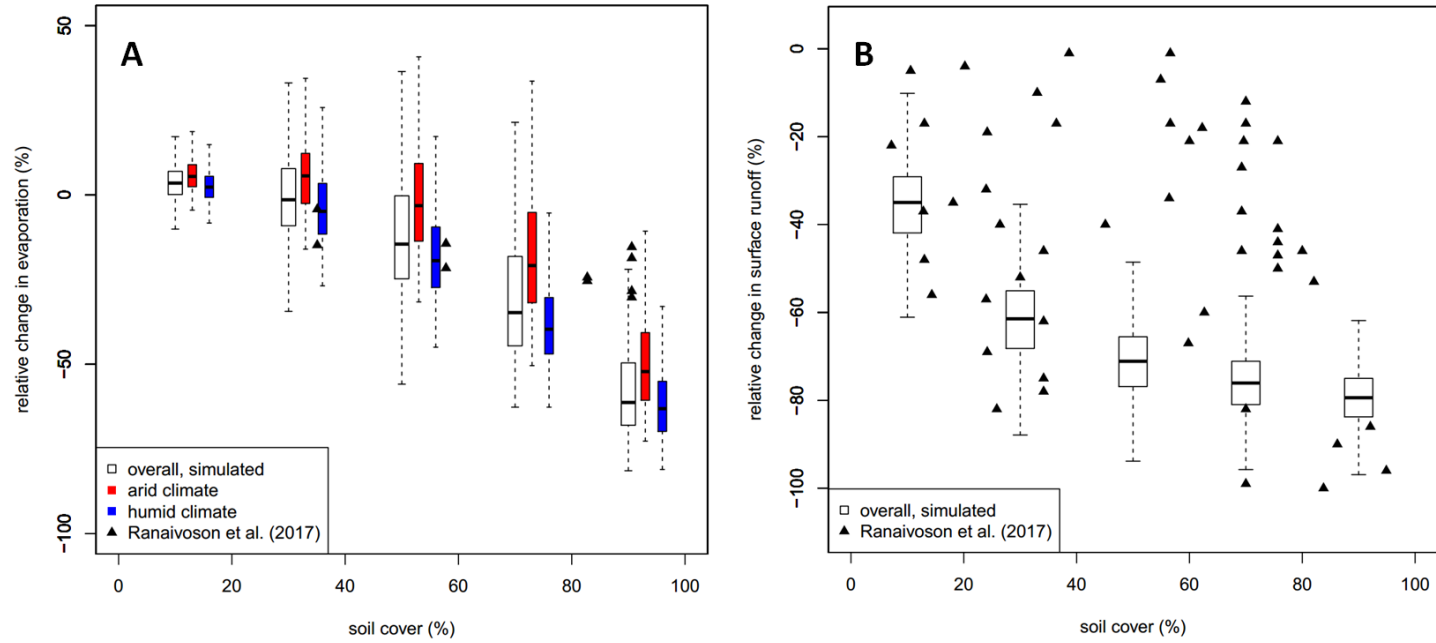
Figure 4: Relative change in evaporation (A) and surface runoff (B) relative to soil cover from surface residues for different soil cover values of 10, 30, 50, 70 and 90% (simulation NT_R_bs1 to NT_R_bs5 vs NT_NR_bs, respectively). For better visibility, the red and blue boxplots are plotted next to the overall boxplots, but correspond to the soil cover value of the overall simulation (empty boxes).
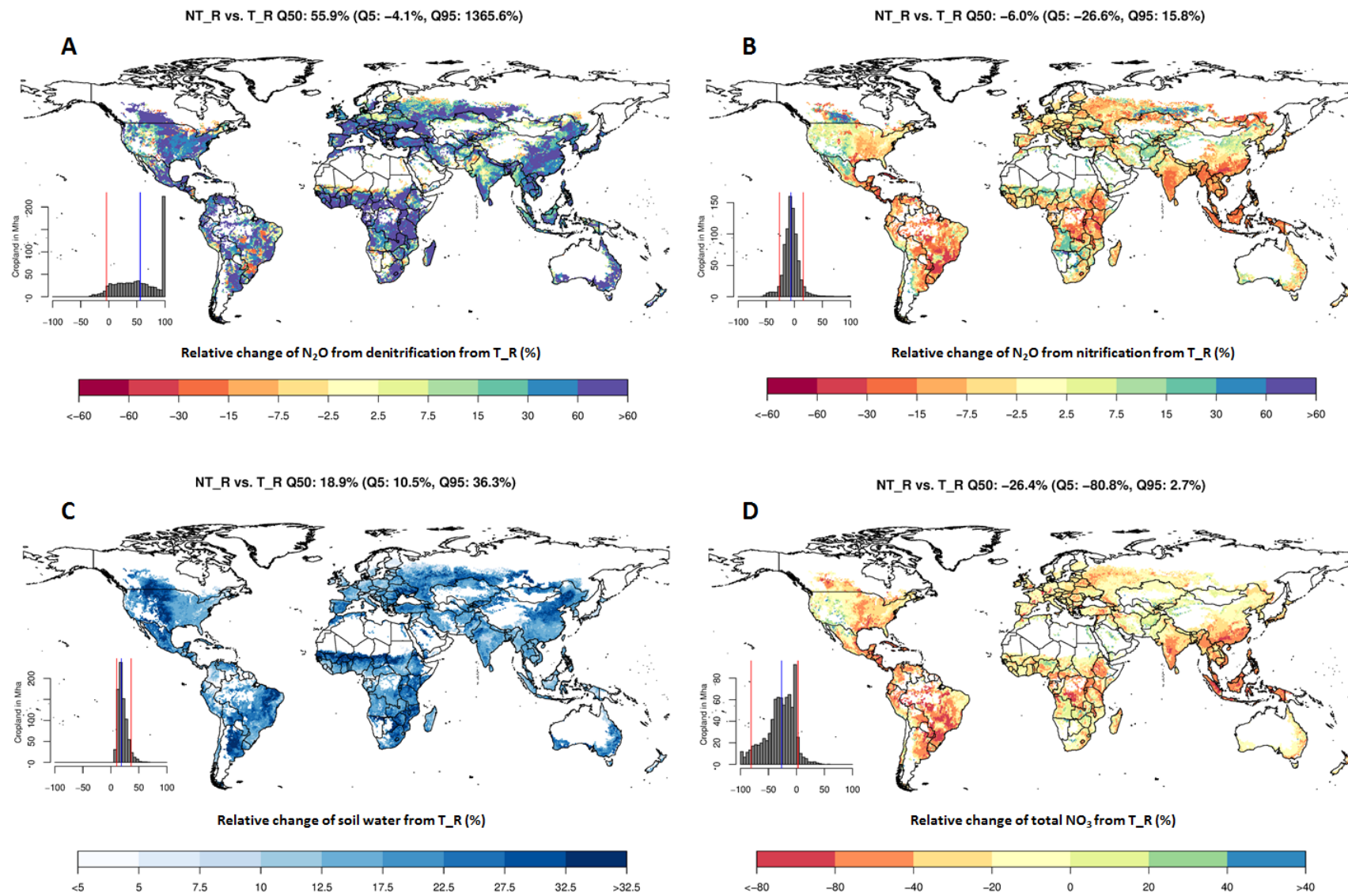
Figure 5: Relative changes for the average of the first three years of NT_R vs. T_R for denitrification (A), nitrification (B), soil water content (C) and NO_3^- (D).